ANTIMICROBIAL ACTIVITY OF CATIONIC ANTISEPTICS IN LAYER-BY-LAYER THIN FILM ASSEMBLIES

A Thesis

by

CHARLENE MYRIAH DVORACEK

Submitted to the Office of Graduate Studies of
Texas A&M University
in partial fulfillment of the requirements for the degree of

MASTER OF SCIENCE

May 2009

Major Subject: Mechanical Engineering

ANTIMICROBIAL ACTIVITY OF CATIONIC ANTISEPTICS IN LAYER-BY-LAYER THIN FILM ASSEMBLIES

A Thesis

by

CHARLENE MYRIAH DVORACEK

Submitted to the Office of Graduate Studies of
Texas A&M University
in partial fulfillment of the requirements for the degree of

MASTER OF SCIENCE

Approved by:

Chair of Committee,	Jaime Grunlan
Committee Members,	Michael Benedik
	Xinghang Zhang
Head of Department,	Dennis O'Neal

May 2009

Major Subject: Mechanical Engineering

ABSTRACT

Antimicrobial Activity of Cationic Antiseptics in Layer-by-Layer Thin Film Assemblies.

(May 2009)

Charlene Myriah Dvoracek, B.S., Rose-Hulman Institute of Technology

Chair of Advisory Committee: Dr. Jaime Grunlan

Layer-by-layer (LbL) assembly has proven to be a powerful technique for assembling thin films with a variety of properties including electrochromic, molecular sensing, oxygen barrier, and antimicrobial. LbL involves the deposition of alternating cationic and anionic ingredients from solution, utilizing the electrostatic charges to develop multilayer films. The present work incorporates cationic antimicrobial agents into the positively-charged layers of LbL assemblies. When these thin films are exposed to a humid environment, the antimicrobial molecules readily diffuse out and prevent bacterial growth. The influence of exposure time, testing temperature, secondary ingredients and number of bilayers on antimicrobial efficacy is evaluated here. Additionally, film growth and microstructure are analyzed to better understand the behavior of these films.

The antimicrobial used here is a positively-charged quaternary ammonium molecule (e.g. cetyltrimethylammonium bromide [CTAB]) that allow assemblies to be made with or without an additional polycation like polydiallyldimethylamine. While films without this additional polymer are effective, they do not have the longevity or

uniformity of films prepared with its addition. All of the recipes studied show linear growth as a function of the number of bilayers deposited and this growth is relatively thick (i.e. > 100 nm per bilayer). In general, 10-bilayer films prepared with CTAB and poly(acrylic acid) are able to achieve a 2.3 mm zone of inhibition against *S. aureus* bacteria and 1.3 mm against *E. coli* when test are conducted at body temperature (i.e. 37^{o}C). Fewer bilayers reduces efficacy, but lower test temperatures improve zones of inhibition. As long as they are stored in a dry atmosphere, antimicrobial efficacy was found to persist even when films were used four weeks after being prepared. The best films remain effective (i.e. antimicrobially active) for 4-6 days of constant exposure to bacteria-swabbed plates. This technology holds promise for use in transparent wound bandages and temporary surface sterilization.

DEDICATION

To my mother who has always inspired me to strive for my absolute best

ACKNOWLEDGEMENTS

I would like to thank my committee chair, Dr. Grunlan, for his continual guidance during my time at Texas A&M University, and my committee members, Dr. Benedik and Dr. Xhang, for their support throughout the course of this research.

Additionally, I would like to thank my friends, colleagues, and the department faculty and staff for making my experience at Texas A&M University excellent. I want to extend my sincere gratitude to the National Science Foundation for their support through the Graduate Research Fellowship and also the Texas Engineering Experience Station (TEES).

Finally, thanks to my mother and brothers for their encouragement and love.

NOMENCLATURE

LbL	Layer-by-layer
L-B	Langmuir-Blodgett
BL	Bilayer
CTAB	Cetyltrimethylammonium bromide
PDDA	Polydiallyldimethylammonium chloride
PAA	Polyacrylic acid
PSS	Polystyrene sulfonate
PEI	Polyethyleneimine
PET	Polyethylene terephthalate
PS	Polystyrene
QCM	Quartz Crystal Microbalance
AFM	Atomic Force Microscope
DDSA	Dodecenylsuccinic anhydride
BDMA	Benzyldimethylamine
TEM	Transmission Electron Microscope
KB	Kirby Bauer
ZOI	Zone of inhibition
FDA	U.S. Food and Drug Administration

TABLE OF CONTENTS

Page

ABSTRACT iii

DEDICATION v

ACKNOWLEDGEMENTS vi

NOMENCLATURE vii

TABLE OF CONTENTS viii

LIST OF FIGURES ix

CHAPTER

I INTRODUCTION 1

II FILM GROWTH AND MICROSTRUCTURE 8

Introduction 8
Experimental 8
Results and Discussion 10
Conclusion 20

III ANTIMICROBIAL EFFICACY 21

Introduction 21
Experimental 21
Results and Discussion 22

IV CONCLUSIONS AND FUTURE WORK 33

Conclusions 33
Future Work 33

REFERENCES 36

VITA 44

LIST OF FIGURES

Page

Figure 1. Schematic of the LbL process that involves alternately dipping a substrate in aqueus solutions containing cationic and anionic ingredients, with rinsing and drying between each deposition. The schematic of the resulting thin film, shown at the bottom, represents build up using a cationic surfactant and anionic polymer. 2

Figure 2. Layer-by-layer assembly with clay can be used to create artificial nacre [36], as seen in this image (a), or it can be used to encapsulate drugs (b) [34]. 4

Figure 3. Chemistry of quaternary ammonium compounds: hexamethylenetetramine (a), cetylpyridinium (b), and hexadecyltrimethylammonium (c). Molecule (a) is an example of an antimicrobial peptide, and molecule (c) is the focus of the present work. 6

Figure 4. Schematic of LbL thin film with an antimicrobial agent included in the cationic layer. 7

Figure 5. A comparison of strong and weak polyelectrolyte systems here demonstrates PDDA-PAA is best for this research. This held true in both ellipsometry (a) and QCM (b). 11

Figure 6. In addition to crystal removal, the flow (a) and dip (b) methods were analyzed to achieve the most accurate QCM data. 12

Figure 7. Comparison of three techniques used to measure LbL deposition using a QCM. The 'dip method' where the entire system undergoes the LbL process, gives the most reliable results. 13

Figure 8. Film mass as a function of the number of layers deposited, as measured with QCM (a). Comparison of QCM to profilometry measurements to confirm the QCM growth trend (b). 15

Figure 9. AFM height images of CTAB/PAA (a) and PDDA+CTAB/PAA (b) 10BL film surfaces. 16

Page

Figure 10. AFM height images of CTAB/PAA films prepared with 5mM CTAB solutions and 1 minute (a) and 30 minute deposition times (c), and 10mM CTAB solutions with 1 minute (b) and 30 minute (d) deposition times. 17

Figure 11. TEM cross-sections of CTAB/PAA (a) and PDDA+CTAB/PAA (b) 10-BL films on polystyrene. 19

Figure 12. A CTAB/PAA 10-BL TEM micrograph reveals a full cross-section of the film. This film again shows a splotchy appearance indicating interdiffusion at deposition and allows measurment of thickness. 19

Figure 13. The Kirby-Bauer test evaluates the antimicrobial efficacy of the LbL films. Disks with LbL films are placed on a bacteria coated agar plate and incubated. The resulting ring of no antibacterial growth (shown above) is the zone of inhibition, which is the measure of antimicrobial efficacy. 23

Figure 14. Zone of inhibition as a function of CTAB concentration for 10-BL CTAB/PAA films. The observed leveling of ZOI prompted the use of 5mM antimicrobial films for all additional studies. 24

Figure 15. Zone of inhibition as a function of PET disk size for 10-BL CTAB/PAA films. From this point forward, all disks used are 0.375 inches. 24

Figure 16. Chemical structures of the three different antimicrobial agents tested in this work: cetyltrimethylammonium bromide (CTAB) (a), cetyltrimethylammonium chloride (CTAC) (b), and cetyltrimethylammonium hydrogen sulfide (CTAHS) (c). 25

Figure 17. Zone of inhibition for 10-BL films with varying antimicrobial agents. No ZOI is observed for CTAHS because it does not build into the assembly. 26

Figure 18. Zone of inhibition for 10 and 20-bilayer films with or without PDDA in the cationic layers. Additional bilayers do not enhance PDDA+CTAB/PAA efficacy, but they do increase efficacy of CTAB/PAA films. 27

Page

Figure 19. Zone of inhibition as a function of number of PDDA+CTAB/PAAbilayers deposited. Error bars reflect maximium and minimum measured zones of inhibition. 28

Figure 20. The ability of CTAB to diffuse through the system was evaluated by building a film with CTAB only in the lower 5-BL using a PDDA+CTAB/PAA film. Results were comparable within error to a 5-BL film constructed with the same amount of antimicrobial. Error bars reflect maximium and minimum zones of inhibition. 29

Figure 21. Zone of inhibition as a function of temperature for 10-BL PDDA+CTAB/PAA films. Larger ZOI at lower temperature is attributed to slower bacterial growth and longer time for CTAB diffusion. 30

Figure 22. Zone of inhibition as a function of storage time for 10-BL PDDA+CTAB/PAA films. Prior to testing, films were stored in a dry environment. 31

Figure 23. Zone of inhibition as a function of days of exposure to KB plates for 10-BL films. Both PDDA+CTAB/PAA and CTAB/PAA films were evaluated to determine how long antimicrobial release will be sustained when in use. 32

Figure 24. Methods to increase antimicrobial film longevity are presented. Altering polymer chemistry can lead to denser films which could slow diffusion out of films (a). Alternately, increasing the number of bilayers (b) increases the amount of antimicrobial in the films and could therefore improve efficacy over time. 35

CHAPTER I

INTRODUCTION

Langmuir's discovery that surfaces could be made to adsorb monolayers of molecules initiated the field of thin film technology [1]. With the more recent advent of technologies geared toward thin film characterization and manipulation, Langmuir-Blodgett (L-B) and related technologies have grown in popularity [2]. Despite their promise, L-B films have several problems for practical applications. In addition to the high costs associated with this method, substrates used must be regular in shape and have smooth, homogeneous surfaces [3]. Moreover, these films have limited stability when subjected to solvents or thermal treatments, and defects in lower layers continue throughout the film (i.e. they cannot be easily covered/healed) [4]. It was for these reasons that many researchers attempted to improve upon this concept.

Iler built upon the L-B concept by creating multilayer films with positively and negatively charged particles [5]. In the early nineties, Decher further developed this idea by creating the formal layer-by-layer (LbL) assembly process [6-8]. In this process, a substrate is alternately dipped into aqueous solutions containing charged ingredients as shown in Figure 1, building a film through electrostatic attractions. LbL assembly is a self-healing process, as defects are erased with sequential buildup of layers [4], and films with a seemingly unlimited number of layers can be created [9]. Hydrogen-bonding and other types of van der Waals attractions can also act as the driving force to build LbL

This thesis follows the style of Biomaterials.

assemblies [10-12], but electrostatic-based deposition remains the predominant mechanism [5, 13-16]. Each positive and negative pair deposited is known as a bilayer (BL), which is typically 1-100 nm thick [13, 17]. Significant interpenetration between layers is often realized in this method, yielding a "fuzzy" microstructure [4, 18]. Analysis of this interpenetration has shown that the thickness of the layer impacts the magnitude of interpenetration [19]. These films are highly tailorable by altering pH [15, 20], ionic strength [14, 20], chemistry [21], and molecular weight [16, 22]. Additionally, film properties can be tailored by adding small amounts of additives to the deposition solution. These additives include clay [23-25], viruses [26], colloidal particles [27, 28], or antimicrobial agents [29, 30].

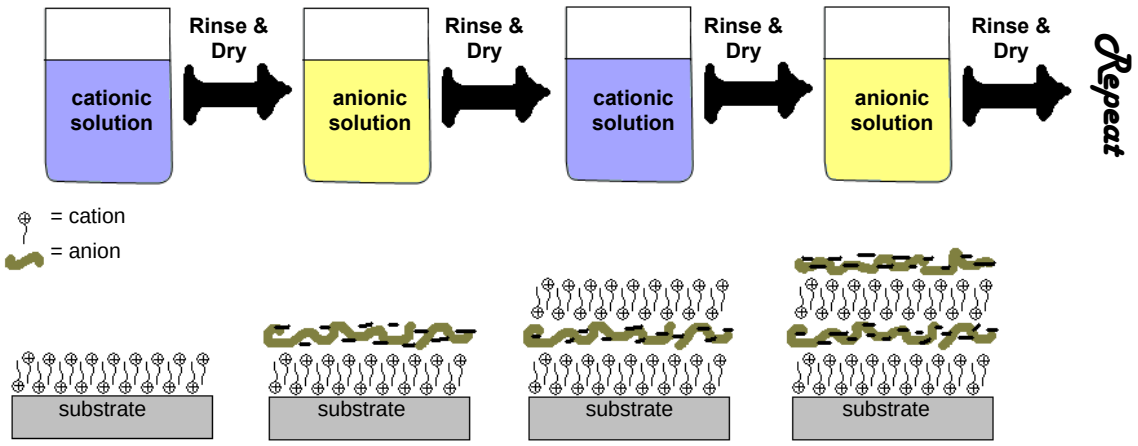

Figure 1. Schematic of the LbL process that involves alternately dipping a substrate in aqueous solutions containing cationic and anionic ingredients, with rinsing and drying between each deposition. The schematic of the resulting thin film, shown at the bottom, represents build up using a cationic surfactant and anionic polymer.

The layer-by-layer technique has been used to make thin films for antireflection [31], battery electrolytes [32], and drug delivery [33, 34]. The inherent anionic charge of DNA makes it ideal for incorporation into these assemblies, which can yield selective immobilization suitable for biosensors [35]. The addition of small molecules or nanoparticles, added to either the cationic or anionic mixtures, can impart different characteristics or properties to the film [29]. Some examples of these uses can be seen in Figure 2. Clay particles, for example, have been used to create artificial nacre [36] and films with gas barrier properties [24]. The addition of bioactive molecules into these films can make them reservoirs for drug delivery or bioreactors [37]. Adding antimicrobial agents to one of the charged solutions results in films capable of killing bacteria on their surface [29]. Incorporating these antimicrobial molecules into thin coatings is advantageous because greater transparency may allow for monitoring bacterial growth beneath the coating. Additionally, the antimicrobial agents can be incorporated in their ionic form in these films. Evidence suggests that antimicrobial action occurs primarily in this charged state [38, 39], eliminating the need for an activation step. This could provide greater effectiveness at lower concentration than in other systems where antiseptics are incorporated as uncharged solids or salts [29].

The addition of antiseptic agents could be useful in applications such as food packaging [40-43], wound dressing [44], household sanitation [45, 46], and medical devices [47, 48]. In fact, the most common reason for modern implants to fail is infection [49]. It is for this reason that significant research effort has focused on developing effective antimicrobial compounds. Silver particles are known to kill a broad

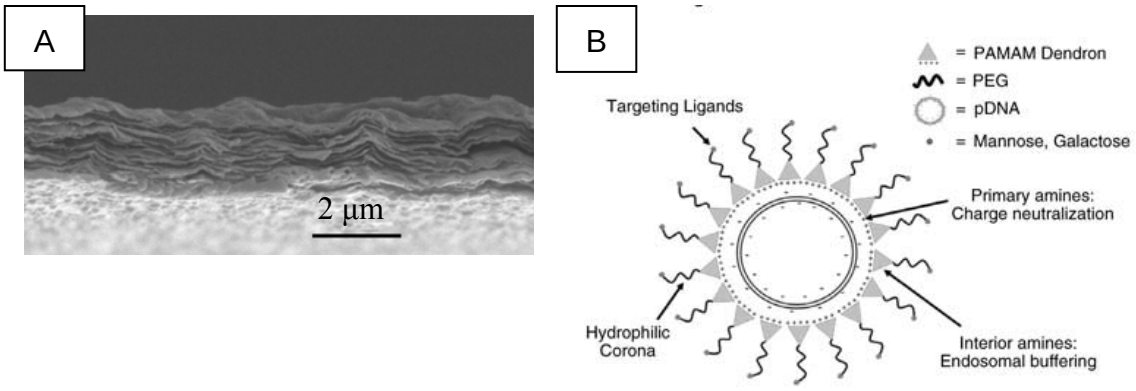

Figure 2. **Layer-by-layer assembly with clay can be used to create artificial nacre [36], as seen in this image (a), or it can be used to encapsulate drugs (b) [34].**

array of infectious bacteria, making them the most widely used antimicrobial agent [48, 50-53]. Antimicrobial polymers have also gained attention in recent years, but they tend to have weaker antimicrobial efficacy than their monomer counterparts [49, 54, 55]. Other widely used antiseptics include iodine [56], quaternary ammonium compounds [57, 58], and antibiotics [59, 60]. The body's innate immune response system has evolved into one of the most powerful antimicrobial systems, leading to natural compounds that can also fight microbes. Antimicrobial peptides, for example exhibit clustering of hydrophobic and cationic amino acid regions [61], as shown in Figure 3(a). This is very similar to the cationic surfactants used in this study. Cetyltrimethylammonium bromide (CTAB) has emerged as one of the most popular antimicrobial surfactants [29, 62, 63] and is the focus of this work.

Antimicrobials have four primary mechanisms of action: hindrance of cell membrane, hindrance incerance of protein, hindrance of nucleic acid synthesis, and inhibition of cell membrane function [64]. While there is some evidence that all of these mechanisms contribute to the antimicrobial activity of the quaternary ammonium

compounds studied here, the overwhelming mode of action is inhibition of cell membrane function [65, 66]. Denyer and Hugo did studies using CTAB to target *S. aureus,* which confirmed the increase in membrane permeability that allowed seepage from the bacterial cell and cell death [67].

Studies of quaternary ammonium compounds as antimicrobial agents began in 1915 with the work of Jacobs and coworkers on hexamethylenetetramine [68-75]. After that time, advances in this field yielded less toxic yet more potent antimicrobials. In 1935, another major advance took place when Domagk showed that long-chain quaternary ammonium salts had antimicrobial activity, further improving antimicrobial efficacy [76]. Some common quaternary ammonium compounds can be seen in Figure 3. When the structure of Figure 3(c) is paired with an anion such as bromide or chloride anions, the result is cetyltrimethylammonium bromide (CTAB) or cetyltrimethylammonium chloride (CTAC), respectively, which were studied here. Recently, CTAB has been used in a variety of studies. The behavior in aqueous solutions was analyzed, specifically looking at the CTAB-water interface [77]. Antimicrobial properties of CTAB were used in wool fabrics [78] and cleaning products [79]. The unique properties of CTAB also enable it to be a directing molecule and thus assist in fabrication of nanoparticles including gold nanorods [80], silver nanorods and nanowires [81], and copper nanoparticles [82]. DNA-CTAB complexes, formed on the basis of charge opposition, have also been studied [83].

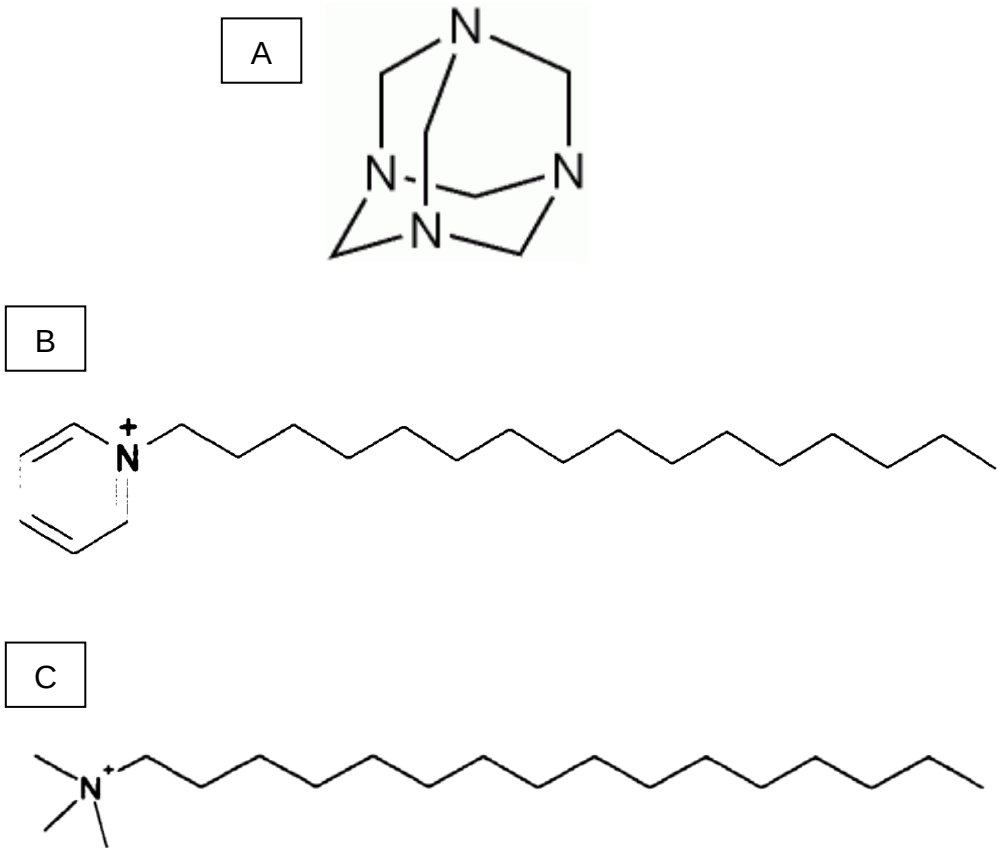

Figure 3. **Chemistry of quaternary ammonium compounds: hexamethylenetetramine (a), cetylpyridinium (b), and hexadecyltrimethylammonium (c). Molecule (a) is an example of an antimicrobial peptide, and molecule (c) is the focus of the present work.**

In the present study, cationic antiseptics (primarily CTAB) were incorporated into the cationic layers of a thin film using LbL assembly, as shown in Figure 4. CTAB has been shown to demonstrate greater antimicrobial efficacy in LbL films than silver [29], making it suitable for further investigation. The following chapters investigate LbL thin films prepared with polydiallyldimethylammonium chloride (PDDA) as the polycation and polyacrylic acid (PAA) as the polyanion. Antimicrobial agents are incorporated into the cationic layer, with or without PDDA. In Chapter II, growth trends

of the various recipes for films were studied and optimized, and the microstructures of the films were investigated. Both the surface structure and final film cross sections were examined. In Chapter III, the effects of number of bilayers, antimicrobial concentration, incubation temperature, chemistry, and time delay after deposition were explored with respect to antimicrobial effectiveness. The antimicrobial efficacy is especially sensitive to temperature and time. Diffusion of CTAB through the thin films is also analyzed. Chapter IV discusses future work with antimicrobials in LbL and suggests other bio-based applications that would benefit from the LbL technique.

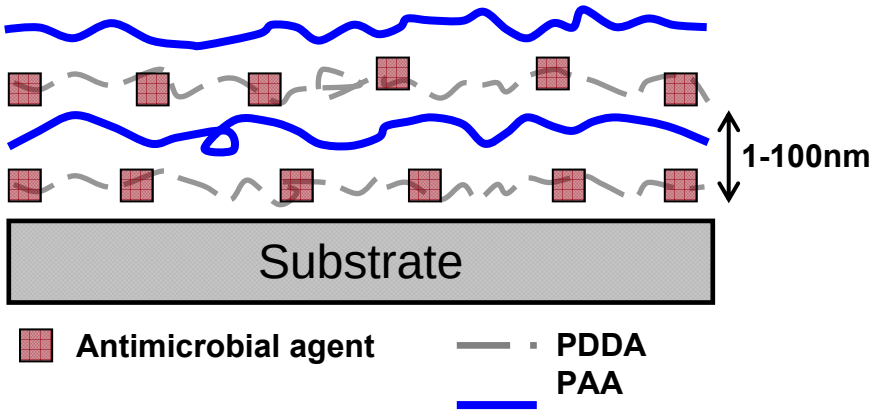

Figure 4. **Schematic of LbL thin film with an antimicrobial agent included in the cationic layer.**

CHAPTER II

FILM GROWTH AND MICROSTRUCTURE

Introduction

Layer-by-layer deposition allows for strategic placement of additives such as antimicrobial agents into thin films and coatings. When placed into a wet environment, these molecules can readily diffuse out of the assembly to produce antimicrobial behavior. The first step to understanding how these systems behave is to understand how they are grown. Film growth and microstructure of these antimicrobial assemblies is examined here.

Experimental

Materials. The anionic deposition solutions contained 0.2 wt% polyacrylic acid (PAA) or 0.2 wt% polystyrenesulfonate (PSS) (Aldrich, St. Louis, MO) with a molecular weight (M_w) of 100,000-200,000 g/mol in deionized water (18.2MΩ). Cationic solutions contained 0.2 wt% poly(diallyldimethylammonium chloride) (PDDA) or 0.2 wt% branched polyethyleneimine (PEI) (Aldrich, St. Louis, MO) unless otherwise noted. The antimicrobial agent, cetyltrimethylammonium bromide (CTAB) (Aldrich, St. Louis, MO), was added to the cationic solution at specified molarities. Solutions with more than 5 mM CTAB were heated to 70°C to achieve complete solvation. Substrates used in this study include 175μm poly(ethylene terephthalate) (PET) (trade name ST505 by DuPont Teijin, Tekra Corp., New Berlin, WI), 125μm polystyrene (PD) (Goodfellow,

Oakdale, PA), and cleaved mica (potassium alumina silicates) disks (Structure Probe, Inc., West Chester, PA).

Film Deposition. In all cases, the substrate was negatively charged, either by using a substrate with an inherent negative charge or corona treatment of an uncharged polymer substrate, such as PET. Prior to corona treatment, the PET and PS films were rinsed with methanol and deionized water and then dried with filtered air, while glass and mica substrates were rinsed with acetone instead of methanol. The cleaned substrates were then dipped alternately in positive and negative solutions to build the film. The initial dip in each solution was five minutes, with subsequent dip times of one minute each. Between each layer, the films were rinsed with deionized water and blown dry with air. Specimens were stored in a desiccator prior to testing.

Film Growth. A Maxtek Research Quartz Crystal Microbalance (RQCM) from Infinicon (East Syracuse, NY), with a frequency range of 3.8-6 MHz, was used in conjunction with 5MHz quartz crystals. The crystal, in its holder, was dipped alternately in the positive (PDDA + antimicrobial) and negative (0.2 wt% PAA) solutions, with frequency shift measured every layer. A Dektak 3 Stylus Profilometer (Neutronix-Quintel, Morgan Hill, CA) was also used to directly measure thickness. Films evaluated using profilometry were deposited onto glass slides. This method gives an absolute measurement of thickness, but it is only accurate beyond a film thickness of approximately 1 μm. Additionally, the profilometry readings were taken upon the completion of each film, while the QCM measurements were taken throughout a film's growth.

Film Characterization. Film surfaces were imaged with a Nanosurf EasyScan 2 Atomic Force Microscope (AFM) (Nanoscience Instruments, Inc., Phoenix, AZ) in dynamic mode with an ACL-A cantilever tip. Sample preparation for the AFM involved deposition onto cleaved mica. The AFM was used to characterize film roughness and uniformity. Cross sections of the assemblies were imaged with a JEOL 1200 EX TEM (JEOL USA Inc., Peabody, MA) at an accelerating voltage of 100kV. PS substrates were used instead of PET to facilitate sectioning. After deposition, the film and substrate were embedded in epoxy resin with a 1:1 anhydride:epoxide (A:E) ratio. This epoxy was comprised of Areldite 502 and Quetal 651 as the epoxy resin, along with dodecenylsuccinic anhydride (DDSA) hardener and benzyldimethylamine (BDMA) accelerator. Using ultramicrotomy, specimens were sectioned down to 70-110 nm thicknesses. These sections were vapor stained on nickel grids using a RuO_4 staining solution prepared by adding 1ml of 10w/v% sodium hypochlorite solution to 0.02 g of $RuCl_3$ [84].

Results and Discussion

Initially, film growth of three different systems of varying polyelectrolyte strength combinations were analyzed (Figure 5). The polyelectrolytes used were polystyrene sulfonate (PSS) (strong, anionic), polyacrylic acid (PAA) (weak, anionic), polyethyleneimine (PEI) (weak, cationic), and polydiallyldimethlyammonium chloride (PDDA) (strong, cationic). Both ellipsometry (Figure 5(a)) and QCM (Figure 5(b)) data revealed PDDA-PAA to have the most stable and greatest growth.

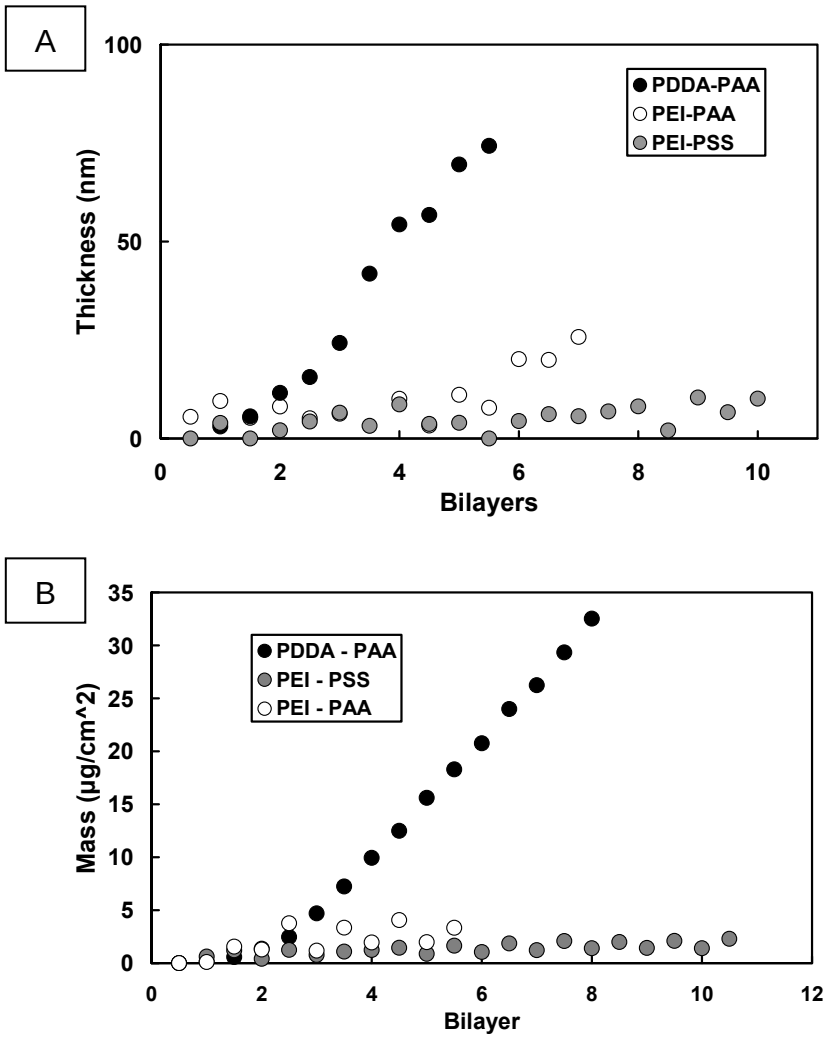

Figure 5. A comparison of strong and weak polyelectrolyte systems here demonstrates PDDA-PAA is best for this research. This held true in both ellipsometry (a) and QCM (b).

With the PDDA-PAA system selected for analysis, the QCM was studied to determine which measurement method gave the most reasonable results. The three techniques investigated were: removal of the crystal from the QCM during the LbL process, using an open faced QCM that allows dipping of the entire crystal and holder for the assembly process, and a closed cell with an inlet and outlet to enable flow of

cationic and anionic fluids through the crystal chamber (see Figure 6). Additionally, QCM was performed by removing the crystal from the holder for dipping. From these studies, the method in which the entire system was dipped was found to be best. Figure 7 summarizes the results using each technique. The flow method data was more erratic than the other two methods and yielded a much heavier deposition. Errors with this method were expected to be significant, as not all of the ingredients could be flushed out between steps. Minor buildups of precipitates (e.g., complexation of PDDA and PAA) may have contributed to the heavy deposition observed. It should be noted that the crystal removal method is the only one where the film is deposited on both sides of the crystal. Therefore, masses recorded for this method are roughly double what is seen in the dip method. Both the dip and the crystal removal methods yield accurate data, but problems can occur upon continuous extraction and replacement of the crystal. For higher numbers of dips and overall consistency, the dip method was chosen for this work.

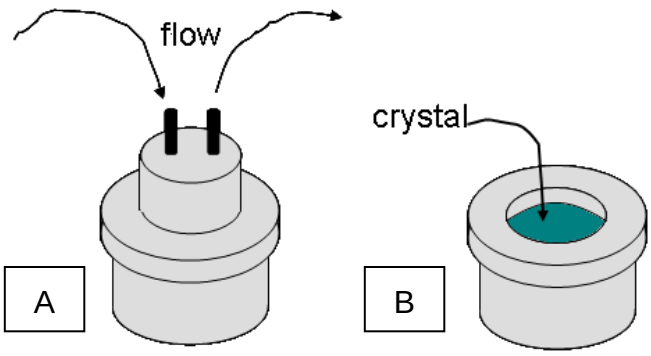

Figure 6. In addition to crystal removal, the flow (a) and dip (b) methods were analyzed to achieve the most accurate QCM data.

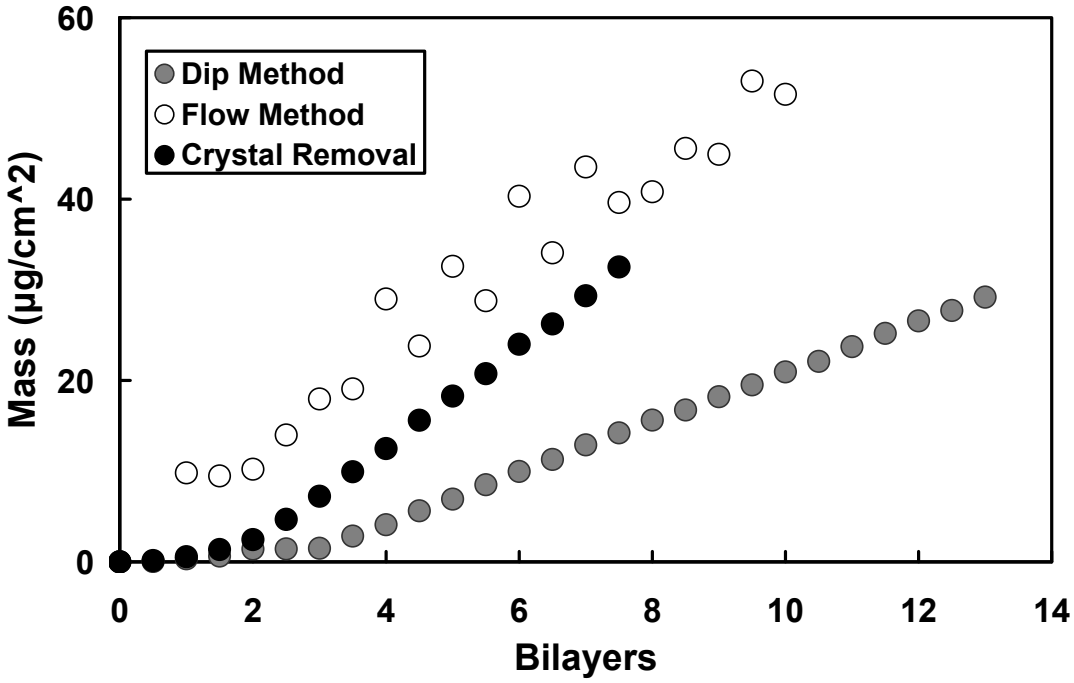

Figure 7. Comparison of three techniques used to measure LbL deposition using a QCM. The 'dip method' where the entire system undergoes the LbL process, gives the most reliable results.

Figure 8(a) shows film growth monitored using QCM. A control system (without the antimicrobial agent) is included to show the influence of CTAB on growth. With the addition of CTAB, growth proceeds at a much higher rate. Additionally, weight variation between PDDA+CTAB/PAA and the CTAB/PAA systems in minimal, suggesting that CTAB deposits to a much greater extent than PDDA. This is not surprising considering the CTAB is a much smaller molecule and likely has greater mobility in solution. Film thickness was measured using profilometry at 7, 10, 15, and 20 bilayers, as shown in Figure 8(b). The growth trend here confirms the trend obtained using QCM. Since the PDDA/PAA films exhibit much slower (thinner) growth, they

were too thin for measurement using profilometry at less than 20-BL and were not analyzed. Again, film growth in the CTAB/PAA system was greater than PDDA+CTAB/PAA. It has been shown that the addition of salts to LbL solutions yields much thicker films [85]. In this system the CTAB is a salt, increasing ionic strength and screening charges on the polymers. Similarly, when the PDDA is removed from the cationic solution, the charge density decreases, and the resulting film is slightly thicker. In the absence of PDDA, rougher films with larger domain structure are generated. It is also possible that CTAB molecules, consisting of a 16-carbon tail and cationic ammonium head group, deposit as something resembling a lipid bilayer found in cell walls (shown schematically in Figure1). This would account for the ability of singly-charged CTAB to generate the charge-inversion necessary to grow in the absence of a highly-charged cation like PDDA. In films with only single ingredients in each layer, film composition in weight or mole percent can be determined. For this analysis, CTAB molecular weight was calculated without bromide because this is removed in aqueous solution. In the case of PAA, repeat unit molecular weight was used. Calculations revealed CTAB/PAA films are 79.9 mol % ± 0.86 mol % PAA and 20.1 mol % ± 0.86 mol % CTAB.

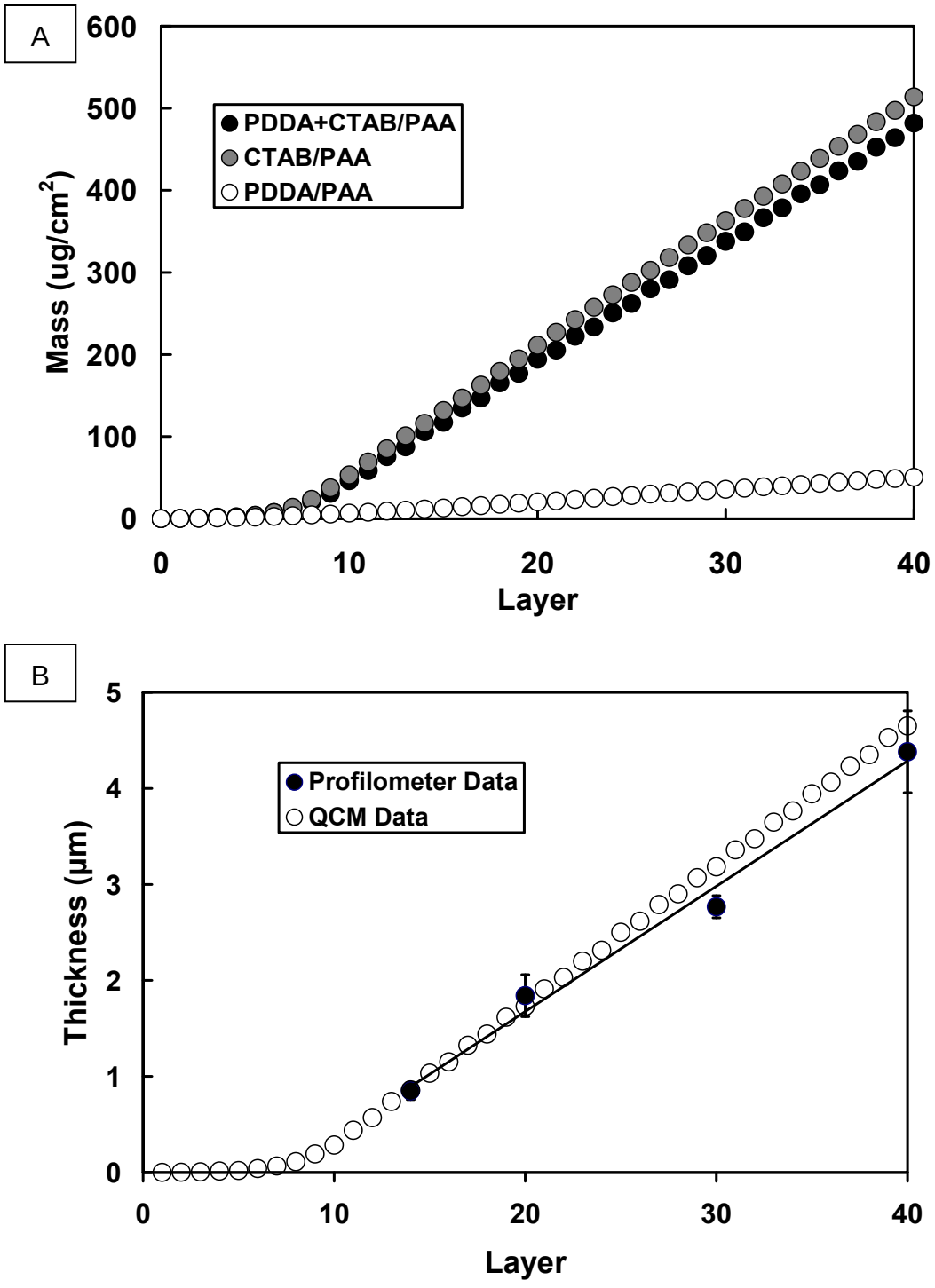

Figure 8. Film mass as a function of the number of layers deposited, as measured with QCM (a). Comparison of QCM to profilometry measurements to confirm the QCM growth trend (b).

The surfaces of the films were analyzed using an AFM, as shown in Figure 9. Comparison of CTAB+PDDA / PAA and CTAB / PAA films reveals a definite structural difference. The system without the polymer in the cationic layer has a much rougher surface. The range of surface height is nearly halved with the inclusion of PDDA. Also worth noting is that this variation in surface height seen in the CTAB/PAA system is on the order of the overall surface height seen previously using profilometry. This data suggests a higher amount of CTAB aggregation without PDDA, revealing better dispersion with the addition of the polymer to the cationic layer. Attempts to use infrared microscopy were inconclusive, but this is to be expected because the IR spot size of 10-15 μm does not provide high enough resolution to distinguish the regions in these films.

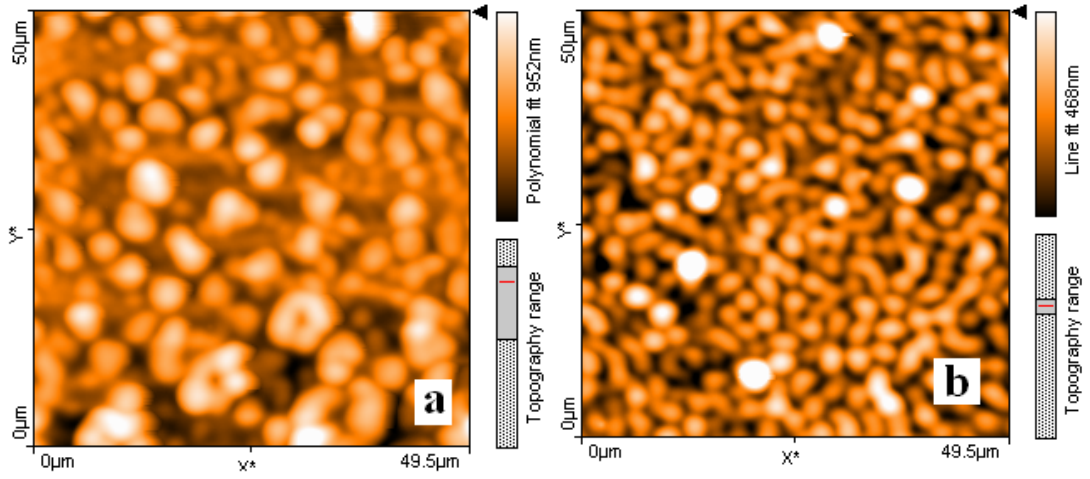

Figure 9. AFM height images of CTAB/PAA (a) and PDDA+CTAB/PAA (b) 10BL film surfaces.

In order to better understand this deposition process, studies of dip time and antimicrobial concentration on the film structure were undertaken. Figure 10 shows

these results by comparing 5mM CTAB cationic solutions with 10 mM CTAB solutions and 1 minute dip times with 30 minute dip times. As dip time was increased, the surface height variation was decreased by almost an order of magnitude for both CTAB concentrations. When concentration was increased, little difference was seen with 30 minute dip times, but smoother films were produced with one minute dips. The increased smoothness in the CTAB/PAA films over longer deposition times may reflect reorganization of CTAB.

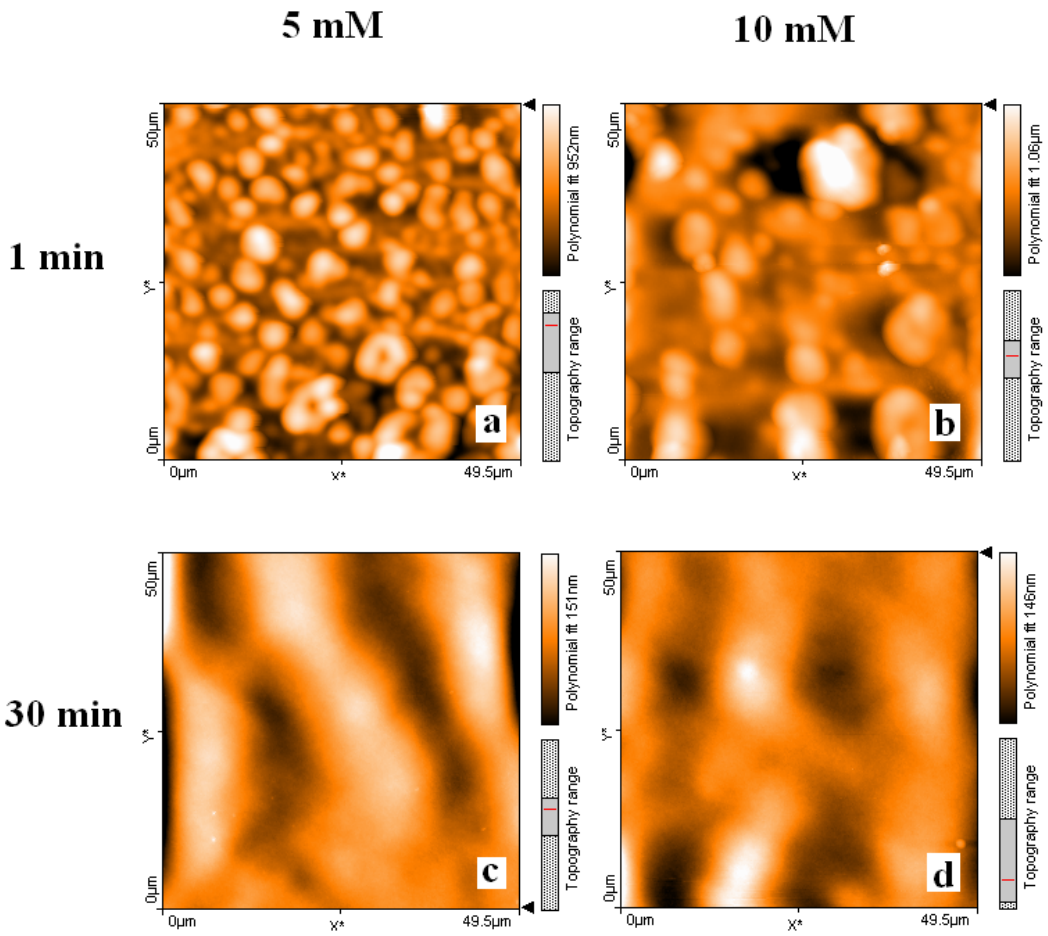

Figure 10. AFM height images of CTAB/PAA films prepared with 5mM CTAB solutions and 1 minute (a) and 30 minute deposition times (c), and 10mM CTAB solutions with 1 minute (b) and 30 minute (d) deposition times.

In Figure 11, 10-BL films deposited on polystyrene, with and without PDDA in the cationic layer, are compared using TEM. A CTAB/PAA film is shown in Figure 11(a) while a PDDS+CTAB/PAA film is shown in Figure 11(b). The films in these micrographs have a mottled appearance, indicating that the layers of the film intertwine and diffuse among each other rather than laying down discretely. These high levels of diffusion during film deposition suggest that CTAB will easily diffuse through the film during use, increasing antimicrobial efficacy. Additionally, the film created with PDDA in the cationic layer shows better uniformity because the PDDA spatially separates CTAB during deposition. While this does not seem to affect initial antimicrobial activity, this may increase film longevity because diffusion out of the film is less clustered. This affects film longevity, consequently affecting reliability, because diffusion out of the film is less sporadic. It is these nano/microstructural characteristics that influence the antimicrobial behavior of these films, as described in the next section.

In addition to understanding microstructure, TEM can confirm film thickness. Generally, films separate during sectioning because they are weakened during water floatation, but occasionally both sides of the section remain close, allowing measurement of film thickness. Figure 12 shows an example of this. An average of 10 measurements across the film indicated film thickness of 818.1 ± 49.9 nm. While this number is smaller than film thicknesses shown during profilometry testing (see Figure 8(b)), high film roughnesses seen in AFM (Fig. 8) indicate that film thicknesses at some locations will be on this scale.

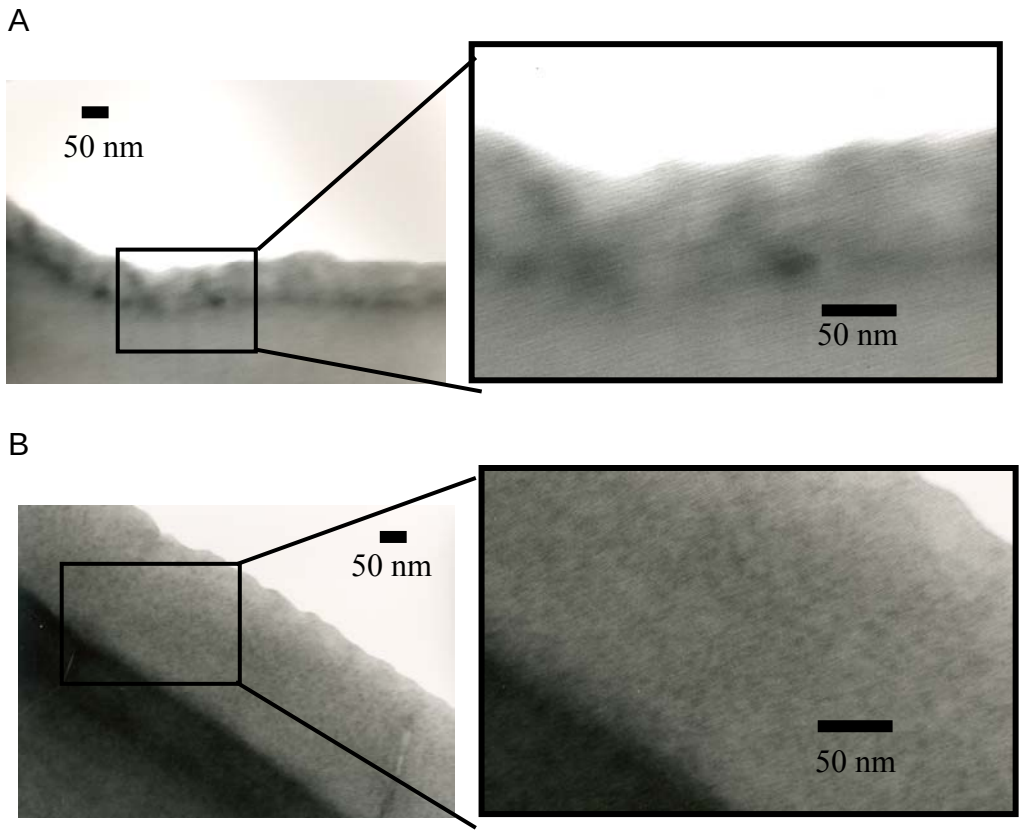

Figure 11. TEM cross-sections of CTAB/PAA (a) and PDDA+CTAB/PAA (b) 10-BL films on polystyrene.

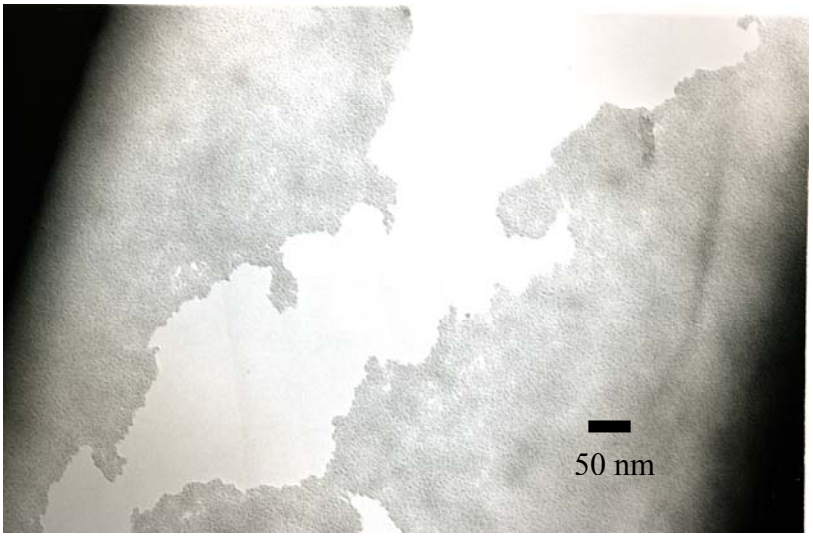

Figure 12. A CTAB/PAA 10-BL TEM micrograph reveals a full cross-section of the film. This film again shows a splotchy appearance indicating interdiffusion at deposition and allows measurment of thickness.

Conclusion

Films made with PDDA/PAA as the base polymeric system for antimicrobial assemblies exhibited the most reliable growth. Films created without the polymeric cation (i.e. CTAB/PAA) demonstrate similar growth, but CTAB seems to cluster in these films, decreasing film uniformity. Imaging of these films with TEM requires a staining procedure to visualize the antimicrobial component. Future work will include microstructural and growth analyses of films with alternative antimicrobials.

CHAPTER III

ANTIMICROBIAL EFFICACY

Introduction

Once film growth and microstructure has been established, as in Chapter II, it is important to investigate the antimicrobial properties of the films. Studying the antimicrobial efficacy reveals diffusion properties of the films because antimicrobial action takes place when the antimicrobial agents diffuse out of the films. This chapter investigates the effects of various factors, including temperature, time, and chemistry on antimicrobial action. Finally, the antimicrobial results are analyzed and compared with the microstructure results from Chapter II.

Experimental

Materials. All deposition materials and substrates are identical to those described in Chapter II. For the antimicrobial testing, 175μm poly(ethylene terephthalate) (PET) (trade name ST505 by DuPont Teijin, Tekra Corp., New Berlin, WI) was used exclusively. Bacterial growth media was from Difco LB Broth solidified with 1.5% bacteriological agar (United States Biologicals, Swampscott, MA). An *Escherichia coli* (*E. coli*) K-12 lab strain MB458 (F-*galK*16 *galE*15 *relA*1 *rpsL*150 *spoT*1 *mcrB*1) and *Staphylococcus aureus* (*S. aureus*), wild type strain, lab strain MB1594, were the bacteria used in testing.

Film Preparation. Films were deposited on PET sheets using the procedure described in Chapter II. After film deposition, disks were cut out of the PET sheets

using punches from O'Brien Consolidated Industries, Inc (Lewiston, Maine). Between film preparation and testing, specimens were stored in a desiccator in order to prevent CTAB leaching out of the film.

Antimicrobial Effectiveness. The effectiveness of the antimicrobial films were tested using a method analogous to the Kirby-Bauer test [86]. The zone of inhibition (ZOI) was evaluated around disks cut from PET (3/8" diameter unless otherwise noted) coated on both sides with the antimicrobial film. An LB petri plate was swabbed with solutions of *E. coli* or *S. aureus* immediately prior to disk placement and incubated for 24 h at 37°C. Figure 13 shows how ZOI was determined. ZOI was recorded for each condition as the average of 8 radial measurements, from the rim of the disk to beginning of bacterial growth, with 2 disks per condition. Reported error is the maximum and minimum ZOI observed. Films were deposited on PET substrates, and accordingly bare PET samples were evaluated as controls. In both the *E. coli* and *S. aureus* tests, the ZOI of the PET alone was zero, indicating that it is not inhibitory. Antimicrobial properties of various films were tested under a variety of conditions that include film composition, number of bilayers, testing temperature, and age of a given film.

Results and Discussion

In the beginning stages of this work, it was important to determine the optimal concentration of CTAB in solution for the layer-by-layer process. Six different solutions were made with CTAB concentrations ranging from 0.1 mM to a supersaturated solution of 100 mM. Figure 14 shows ZOI of films made with these solutions, on both *S. aureus*

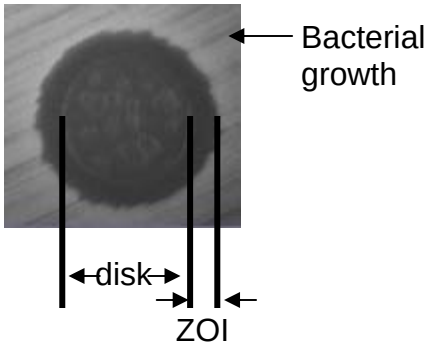

Figure 13. The Kirby-Bauer test evaluates the antimicrobial efficacy of the LbL films. Disks with LbL films are placed on a bacteria coated agar plate and incubated. The resulting ring of no antibacterial growth (shown above) is the zone of inhibition, which is the measure of antimicrobial efficacy.

and *E. coli*, and reveals a leveling in antimicrobial efficacy around 5 mM CTAB. The amount of antimicrobial deposition in layer-by-layer films may become independent of initial concentration once some critical solution concentration is reached, which would explain this leveling. If only a certain maximum amount of antimicrobial can be deposited into a monolayer of the film, eventually increased solution concentration will not lead to increased film concentration or increased film efficacy. These results led to the use of 5 mM antimicrobial solution for all additional studies. This concentration is large enough to reach maximum efficacy.

Additional tests were performed with 5 mM CTAB using various sized antimicrobial disks. Figure 15 shows that each disk size (within error) has the same antimicrobial efficacy regardless of size. Antimicrobial agents are released from the edge of the disks, so the size of disk interior is largely irrelevant in this type of testing. Since ZOI is independent of disk size, 0.375" diameter was chosen for the remainder of testing.

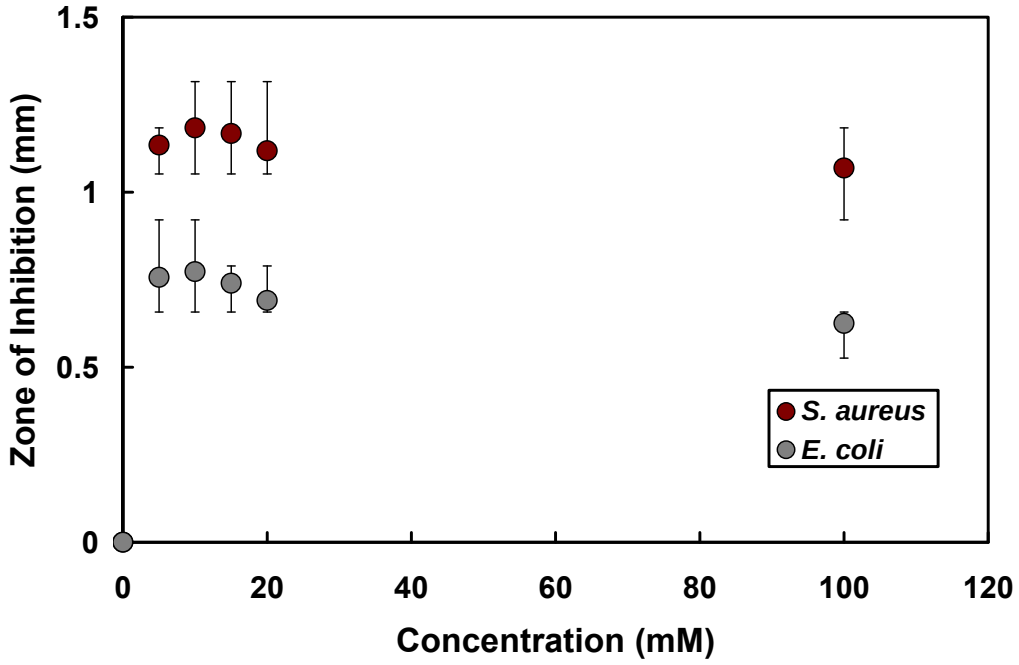

Figure 14. Zone of inhibition as a function of CTAB concentration for 10-BL CTAB/PAA films. The observed leveling of ZOI prompted the use of 5mM antimicrobial films for all additional studies.

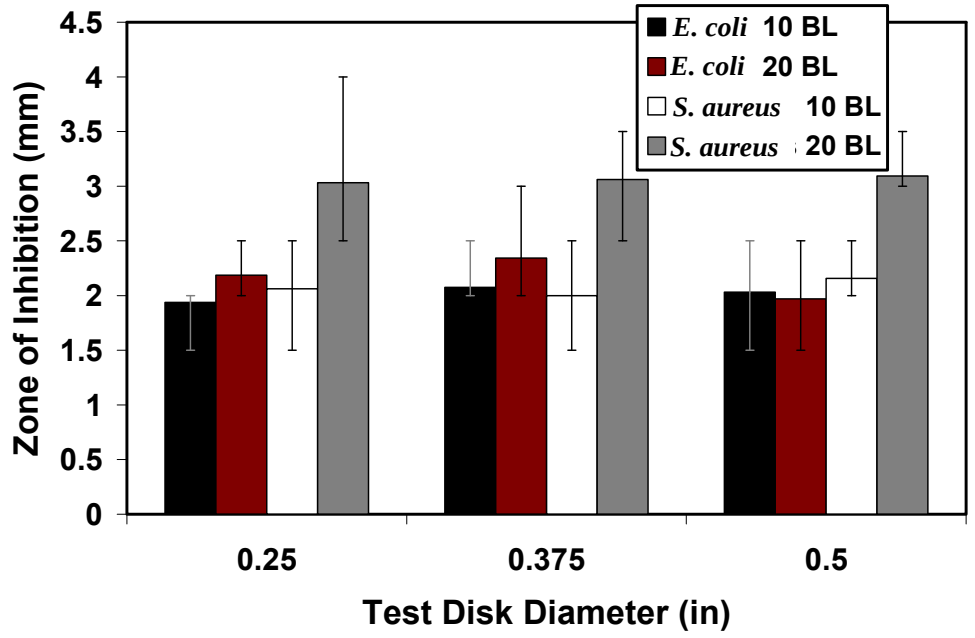

Figure 15. Zone of inhibition as a function of PET disk size for 10-BL CTAB/PAA films. From this point forward, all disks used are 0.375 inches.

Three different cationic quaternary ammonium compounds were examined here: cetyltrimethylammonium bromide (CTAB), cetyltrimethylammonium chloride (CTAC), and cetyltrimethylammonium hydrogen sulfate (CTAHS). The structures of these molecules are shown in Figure 16. These three different chemistries were evaluated using 10-BL films in the standard KB-like test. Figure 17 summarizes the results of this testing. CTAHS did not show any antimicrobial efficacy (i.e. it had a ZOI of zero), while both CTAC and CTAB had virtually identical ZOI's within error. These results can be explained by examining the pKa values of the acids associated with counterions. H_2SO_4 has a higher pKa value (-10) than HBr or HCl (-9 and -7, respectively). More negative pKa values lower the likelihood that these counterions will separate because the bond is too strong to dissociate. When the antimicrobial agent is unable to dissociate, the cationic component will not deposit into the film.

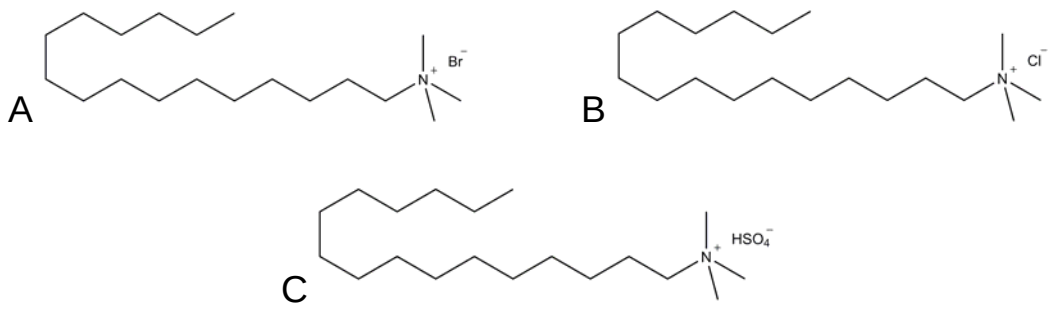

Figure 16. Chemical structures of the three different antimicrobial agents tested in this work: cetyltrimethylammonium bromide (CTAB) (a), cetyltrimethylammonium chloride (CTAC) (b), and cetyltrimethylammonium hydrogen sulfide (CTAHS) (c).

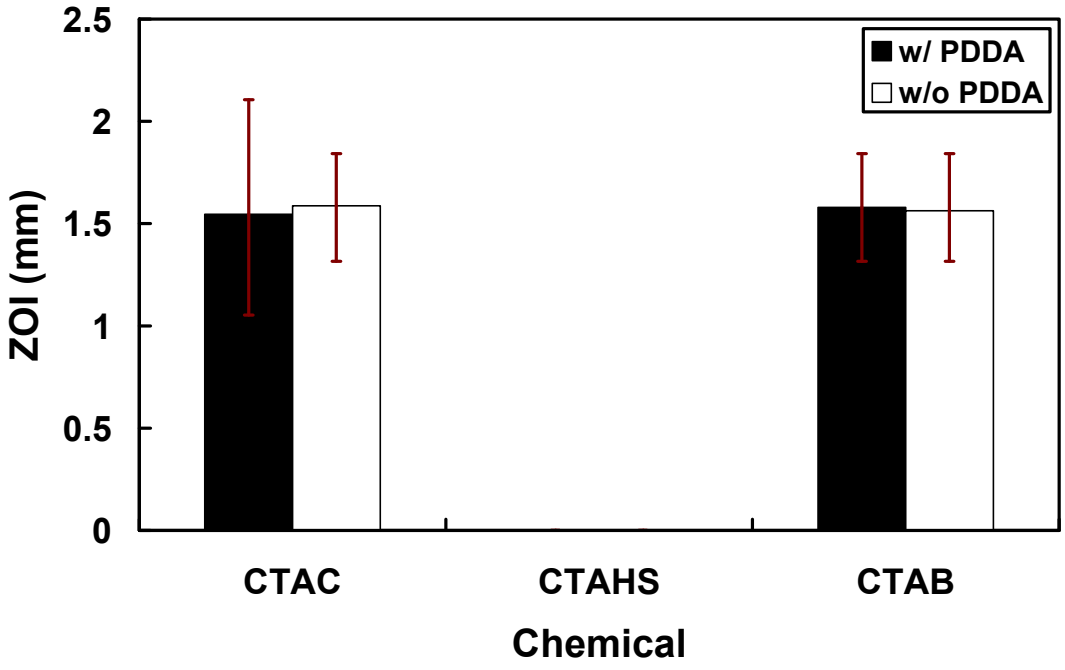

Figure 17. Zone of inhibition for 10-BL films with varying antimicrobial agents tested against *S. aureus*. No ZOI is observed for CTAHS because it does not build into the assembly.

The antimicrobial effectiveness of both PDDA+CTAB/PAA and CTAB/PAA were evaluated with both 10 and 20 bilayers of deposition. At 10-BL, films with PDDA exhibited a greater ZOI (i.e. greater antimicrobial efficacy) than without, and at 20-BL the results were similar, as shown in Figure 18. As was discussed in Chapter II, the PDDA in the cationic layer creates improved dispersion of CTAB in solution. With improved dispersion of CTAB molecules, the antimicrobial range is also increased. With higher numbers of bilayers, the overall stability evens out in solutions prepared without PDDA in the cationic layer, and therefore, these films show similar zones of inhibition. At this testing temperature (37°C), the maximum ZOI observed is approximately 2.3 mm. Increases in antimicrobial efficacy above this point are not

observed due to insufficient time for antimicrobial diffusion prior to antimicrobial growth. Comparison with other data would indicate the 20-BL PDDA/CTAB-PAA film in *S. aureus* would have a larger ZOI, but it reaches this limit.

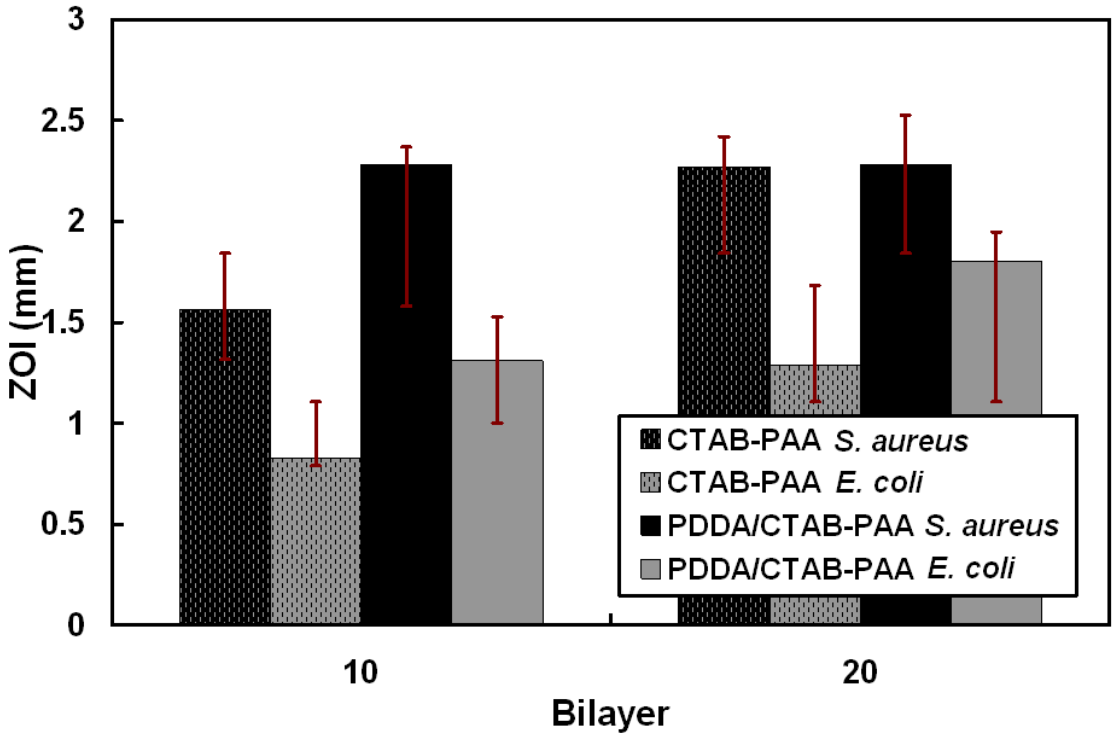

Figure 18. **Zone of inhibition for 10 and 20-bilayer films with or without PDDA in the cationic layers. Additional bilayers do not enhance PDDA+CTAB/PAA efficacy, but they do increase efficacy of CTAB/PAA films.**

It is important to see whether or not the antimicrobial agent diffuses out of merely the top bilayer or if CTAB in lower layers of the film diffuse out as well. By testing various films with different numbers of bilayers, the ability of the bottom layers to contribute to the overall antimicrobial action was tested, as shown in Figure 19. Equal amounts of CTAB were deposited in each of the 9.5 (9 bilayers plus one extra cationic antimicrobial layer) and 10 bilayer films, and the antimicrobial effects are similar. To

further investigate the abilities of CTAB to diffuse through the film, a 10-BL film was constructed with no antimicrobial in the top five bilayers (5BL CTAB+PDDA/PAA followed by 5BL PDDA/PAA). These results, shown in Figure 20, demonstrate that CTAB diffuses through many layers. In fact, a comparison of the 5-BL film and the 10BL film with CTAB only in the lower five bilayers shows equivalent results within error. These results show that the PAA layer does not hinder CTAB diffusion; rather it may act as a protective layer, shielding the antimicrobial beneath from the external environment prior to use.

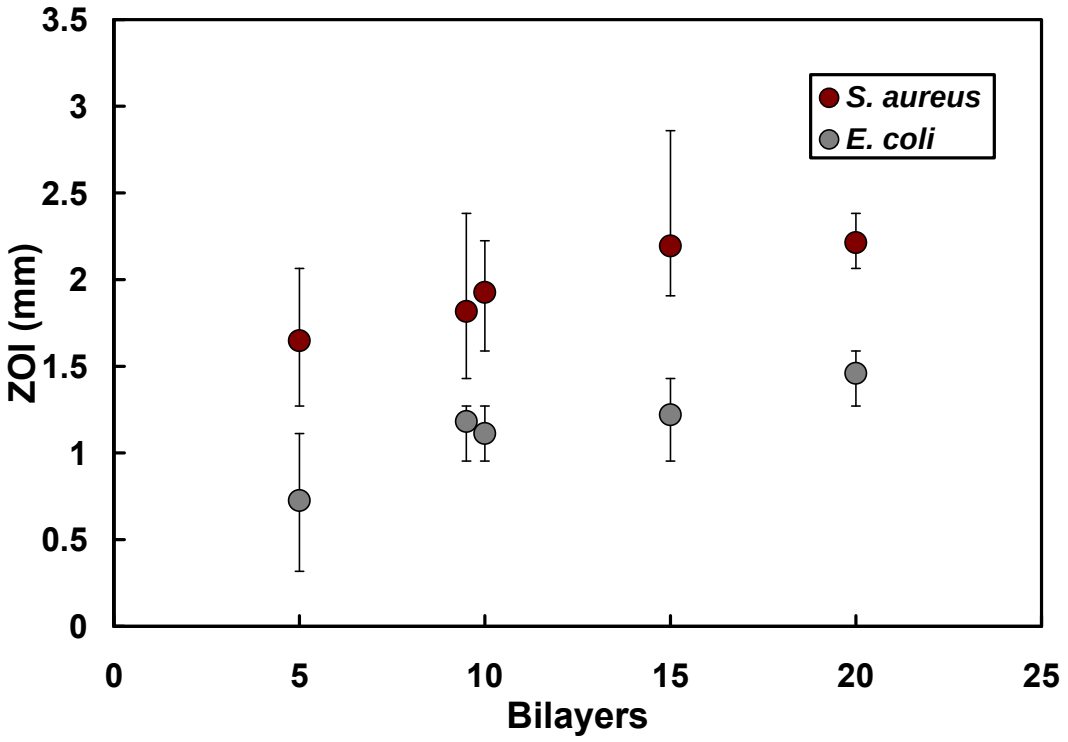

Figure 19. Zone of inhibition as a function of number of PDDA+CTAB/PAA bilayers deposited. Error bars reflect maximum and minimum measured zones of inhibition.

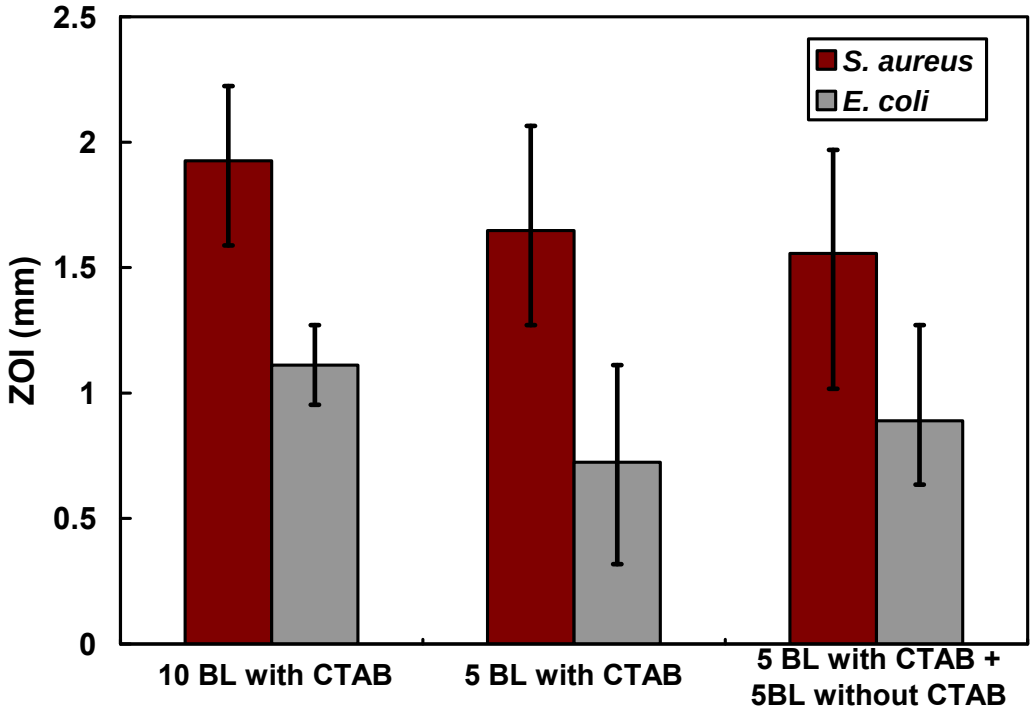

Figure 20. **The ability of CTAB to diffuse through the system was evaluated by building a film with CTAB only in the lower 5-BL using a PDDA+CTAB/PAA film. Results were comparable within error to a 5-BL film constructed with the same amount of antimicrobial. Error bars reflect maximum and minimum zones of inhibition.**

At lower temperatures, bacteria grows more slowly, allowing CTAB more time to diffuse out into the plates during the period of bacteria proliferation. In addition to body temperature (37°C), antimicrobial testing was performed at temperatures of 23°C and 18.2°C. With decreasing temperature, a larger ZOI was observed with both *E. coli* and *S. aureus*, as shown in Figure 21, due to the longer time allowed for CTAB to diffuse. These data suggest that the reason these films do not experience ZOI's greater than 2.5 mm at body temperature is because the antimicrobial cannot travel further than this distance during the bacterial growth period. Once bacteria have established themselves, there will be no subsequent loss of density.

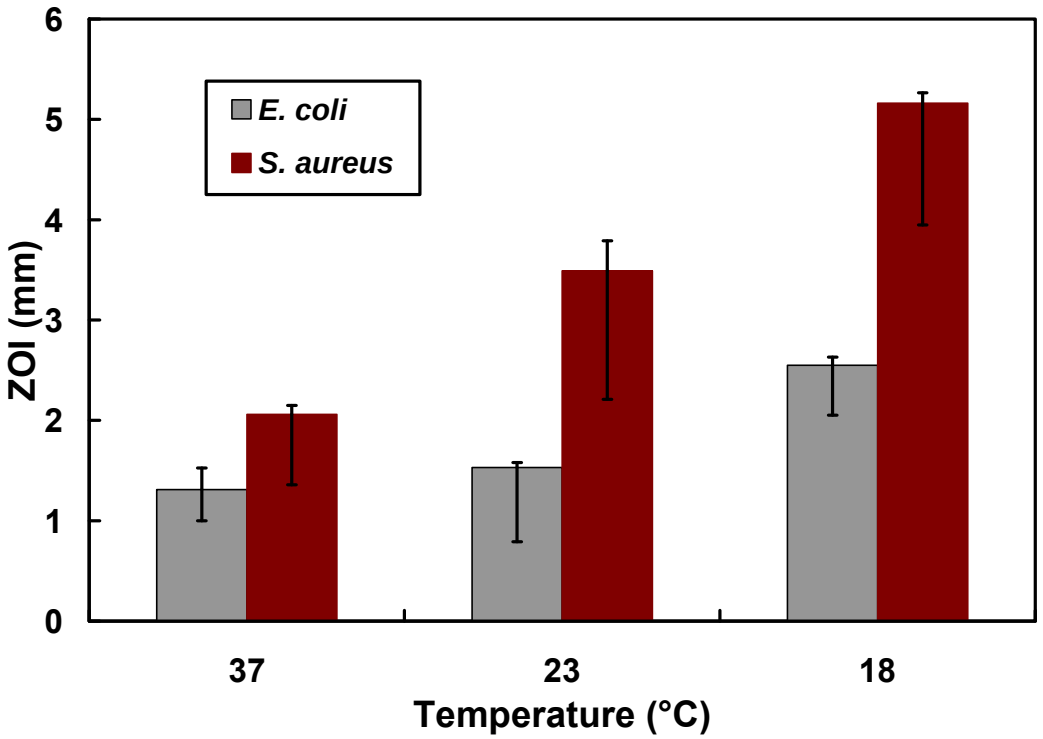

Figure 21. Zone of inhibition as a function of temperature for 10-BL PDDA+CTAB/PAA films. Larger ZOI at lower temperature is attributed to slower bacterial growth and longer time for CTAB diffusion.

The duration of the film efficacy was examined by storing the films in a desiccator for varying lengths of time before testing, as shown in Figure 22. These stored films showed decreased effectiveness initially, but the films maintained significant antimicrobial capacity over the course of four weeks. It is possible that these films rearrange to some equilibrium state after deposition. While antimicrobial activity may not be lost, some CTAB molecules may complex, decreasing their ability to diffuse out. This would explain the initial decrease and eventual leveling of efficacy. It seems that these films can be stored in dry environments for long periods of time without significant loss of antimicrobial efficacy.

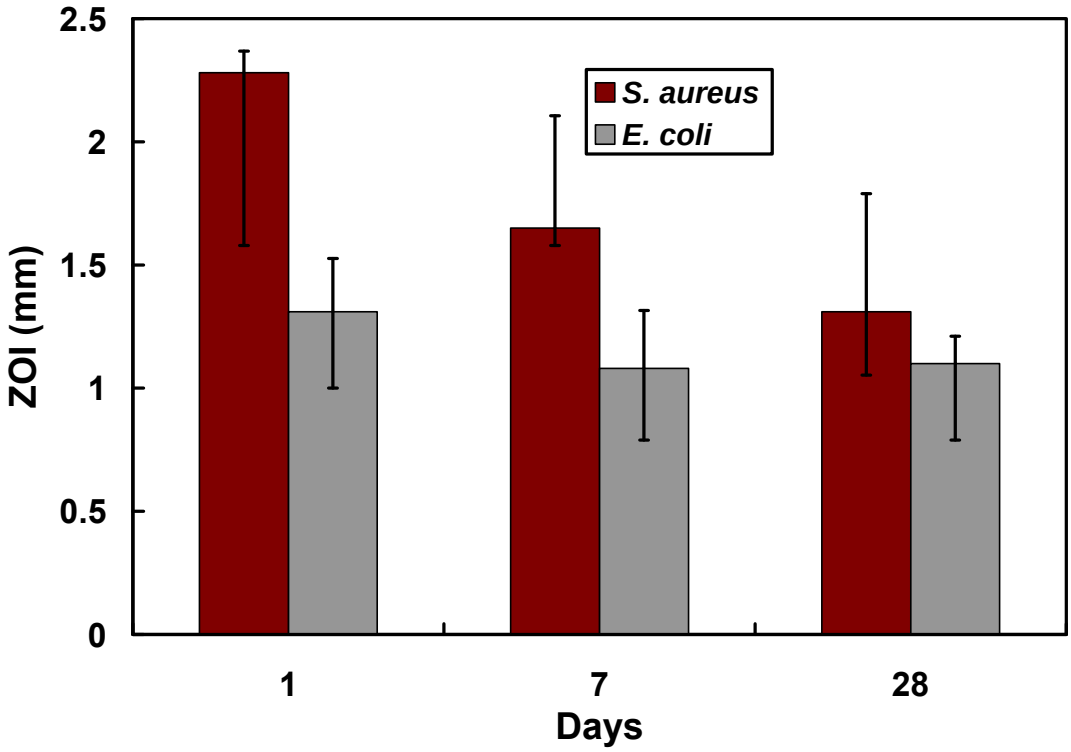

Figure 22. **Zone of inhibition as a function of storage time for 10-BL PDDA+CTAB/PAA films. Prior to testing, films were stored in a dry environment.**

For antimicrobial films, it is important to know how long films will remain active once in use. In this case, duration of efficacy was tested by performing KB-like tests over multiple days where antimicrobial efficacy was evaluated for one initial film by cutting out different disks from this film and evaluating these disks after a varying number of days prior to exposure to bacteria. Films were exposed to the moist humid environment of an uninoculated agar plate in the incubator prior to testing. To ensure continuity in the testing, each day, the antimicrobial disks were removed and placed onto newly swabbed plates. New, clean disks were exposed to bacterial growth each day, but all disks were from the same initial large film, facilitating the study of effective use time.

These 10-BL films of PDDA+CTAB/PAA released CTAB strongly over two days. Results from this test (Figure 23) demonstrate a decreasing effectiveness, with loss of reliability after five days for samples with PDDA in the cationic layer and after four days for samples without. Samples with only CTAB in the cationic layer (i.e. no PDDA) show some antimicrobial action at longer times. Since PDDA acts as a dispersing agent, as seen in both TEM micrographs (Figure 11) and AFM imaging (Figure 9) in Chapter II, KB disks likely came from portions of the film with unequal concentrations of antimicrobial in the CTAB-PAA disks.

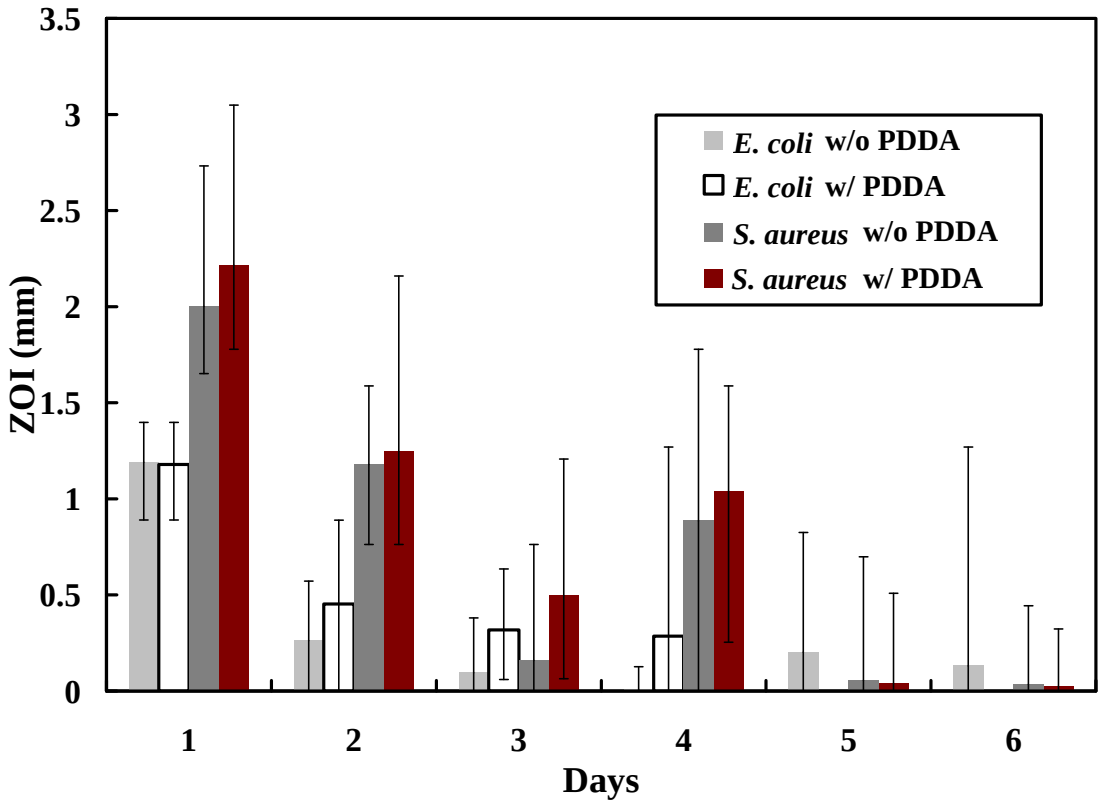

Figure 23. Zone of inhibition as a function of days of exposure to KB plates for 10-BL films. Both PDDA+CTAB/PAA and CTAB/PAA films were evaluated to determine how long antimicrobial release will be sustained when in use.

CHAPTER IV

CONCLUSIONS AND FUTURE WORK

Conclusions

The introduction of antimicrobial agents into LbL films produces antimicrobial properties. Additionally, this work shows that the polycation is not necessary to build the antimicrobial films, but it does assist in film uniformity. The lower uniformity of films without it yields slightly decreased film reliability and antimicrobial efficacy. A discovery of this research was the realization that the CTAB antimicrobial molecules easily diffuse through the LbL films. Using PDDA-PAA as a base for CTAB incorporation produced the highest thickness growth rate, suggesting looser polymer packing that facilitates molecular movement through the system. Comparison of film activity at varying temperatures demonstrated higher bacteria killing abilities at lower temperatures where CTAB had longer time to diffuse out into the system before bacterial growth. These results, in combination with longevity studies, show the best films are effective over a 4-6 day period of activity upon continuous exposure to healthy bacteria. This study lays the groundwork for future studies to improve antimicrobial efficacy and to use LbL assembly to produce films with other types of biological activity (e.g. drug delivery or enzyme stability).

Future Work

Future antimicrobial work will include exploration of alternate biocidal agents for inclusion in the LbL films. Bacteria develop resistance to drugs as they evolve, so it

is important to vary antimicrobials to compensate for this [87]. In order to expand this work for potential use in implantable devices, FDA approved antimicrobials must be explored. The use of hydrophilic antimicrobials could additionally reduce protein adsorption in the body. In the case of implants, these films must retain antimicrobial effectiveness for long periods of time, but the films in this research only stay active for 4-6 days. Future studies will examine methods for lengthening diffusion time, thereby lengthening time of film efficacy. Figure 24 shows some possible methods to improve longevity. Altering polymer chemistry in these LbL films could yield a denser film and thereby a slower diffusion. For instance, the use of a fully charged polyelectrolyte (e.g. polystyrene sulfonate) could decrease the rate of antimicrobial diffusion by increasing the film density [88]. Another method for increasing longevity of film efficacy could involve depositing a higher number of layers. Antimicrobial molecules in the lower layers should take longer to diffuse out, so an analysis of the number of bilayers on efficacy should be performed. For example, a 60-BL film might last longer than the standard 10-BL film used in the work described here.

Other future work focuses on diffusion behavior in LbL assemblies. In the present work, antimicrobial activity was realized as antimicrobial agents diffused out of the film, but the ability of molecules to diffuse out of a film can be used in a variety of applications. Advances in monitoring diffusion out of films could be further utilized in other applications, such as drug delivery. Layer-by-layer films have been studied as a vehicle for drug delivery by encapsulation [89-91] including verification of enzyme stability post-encapsulation [90], but there is still work to be done regarding

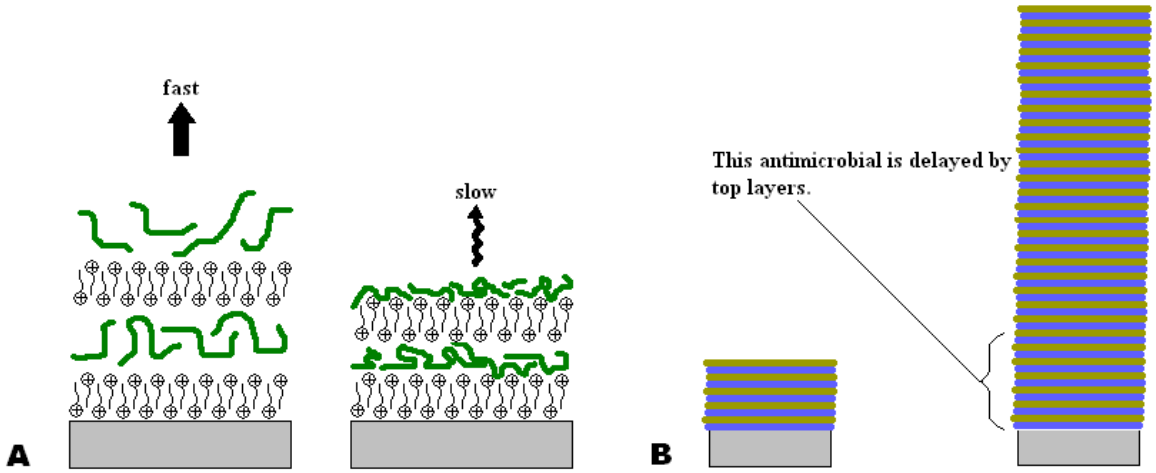

Figure 24. Methods to increase antimicrobial film longevity are presented. Altering polymer chemistry can lead to denser films, which could slow diffusion out of films (a). Alternately, increasing the number of bilayers (b) increases the amount of antimicrobial in the films and could therefore improve efficacy over time.

incorporation of enzymes and other drugs into the layers. In order to fully utilize LbL as a vehicle for enzyme stabilization, enzyme stability must be proven. This can be done by depositing an enzyme such as phosphatase into the films. Upon exposure of the colorimetric substrate p-nitrophenol to these enzyme films, phosphatase acts as a catalyst that triggers a change in substrate color to yellow and confirms enzyme activity. When coupled with an improved understanding of diffusion, confirmation of enzyme activity can lead to a wide variety of biological applications. This could include conversion of water to hydrogen and oxygen as a potential bio-based fuel source [92].

REFERENCES

1. Langmuir I, inventor. US Patent No. U. S. Patent 2,232,539 (General Electric Co.), 1941 February 18.

2. Zasadzinski JA, Viswanathan R, Madsen L, Garnaes J, Schwartz DK. Langmuir-Blodgett-Films. Science 1994 Mar 25;263(5154):1726-1733.

3. Albrecht O, Laschewsky A, Ringsdorf H. Polymerizable built up multilayers on polymer supports. Macromolecules 1984;17(4):937-940.

4. Ciferri A. Supramolecular Polymers. New York: Marcel Dekker, 2000.

5. Iler RK. Multilayers of colloidal particles. Journal of Colloid and Interface Science 1966;21(6):569.

6. Decher G, Hong JD. Buildup of ultrathin multilayer films by a self-assembly process. II: Consecutive adsorption of anionic and cationic bipolar amphiphiles and polyelectrolytes on charged surfaces. International Journal of Physical Chemistry 1991 1991;95(11):1430-1434.

7. Decher G, Hong JD, Schmitt J. Buildup of ultrathin multilayer films by a self-assembly process .3. consecutively alternating adsorption of anionic and cationic polyelectrolytes on charged surfaces. Thin Solid Films 1992 Apr 30;210(1-2):831-835.

8. Hammond PT. Form and function in multilayer assembly: New applications at the nanoscale. Advanced Materials 2004 Aug 3;16(15):1271-1293.

9. Lenahan KM, Wang YX, Liu YJ, Claus RO, Heflin JR, Marciu D, et al. Novel polymer dyes for nonlinear optical applications using ionic self-assembled monolayer technology. Advanced Materials 1998 Aug 3;10(11):853-+.

10. DeLongchamp DM, Hammond PT. Highly ion conductive poly(ethylene oxide)-based solid polymer electrolytes from hydrogen bonding layer-by-layer assembly. Langmuir 2004 Jun 22;20(13):5403-5411.

11. Fu Y, Bai SL, Cui SX, Qiu DL, Wang ZQ, Zhang X. Hydrogen-bonding-directed layer-by-layer multilayer assembly: Reconformation yielding microporous films. Macromolecules 2002 Dec 3;35(25):9451-9458.

12. Kotov NA. Layer-by-layer self-assembly: The contribution of hydrophobic interactions. Nanostructured Materials 1999 Jul;12(5-8):789-796.

13. G. Decher JBS. Multilayer thin films – sequential assembly of nanocomposite materials. Weinheim, Germany: Wiley-VCH, 2003.

14. McAloney RA, Sinyor M, Dudnik V, Goh MC. Atomic force microscopy studies of salt effects on polyelectrolyte multilayer film morphology. Langmuir 2001 Oct 16;17(21):6655-6663.

15. Shiratori SS, Rubner MF. pH-dependent thickness behavior of sequentially adsorbed layers of weak polyelectrolytes. Macromolecules 2000 May 30;33(11):4213-4219.

16. Sui ZJ, Salloum D, Schlenoff JB. Effect of molecular weight on the construction of polyelectrolyte multilayers: Stripping versus sticking. Langmuir 2003 Mar 18;19(6):2491-2495.

17. Jan CJ, Walton MD, McConnell EP, Jang WS, Kim YS, Grunlan JC. Carbon black thin films with tunable resistance and optical transparency. Carbon 2006 Aug;44(10):1974-1981.

18. Decher G. Fuzzy Nanoassemblies: Toward layered polymeric multicomposites. Science 1997 Aug 29;277(5330):1232-1237.

19. Schmitt J, Grunewald T, Decher G, Pershan PS, Kjaer K, Losche M. Internal Structure of layer-by-layer adsorbed polyelectrolyte films - a neutron and x-ray reflectivity study. Macromolecules 1993 Dec 6;26(25):7058-7063.

20. Schoning MJ, Abouzar MH, Poghossian A. pH and ion sensitivity of a field-effect EIS (electrolyte-insulator-semiconductor) sensor covered with polyelectrolyte multilayers. J Solid State Electrochem 2009;13(1):115-122.

21. Mermut O, Barrett CJ. Effects of charge density and counterions on the assembly of polyelectrolyte multilayers. Journal of Physical Chemistry B 2003 Mar 20;107(11):2525-2530.

22. Zhang HY, Wang D, Wang ZQ, Zhang X. Hydrogen bonded layer-by-layer assembly of poly(2-vinylpyridine) and poly(acrylic acid): Influence of molecular weight on the formation of microporous film by post-base treatment. European Polymer Journal 2007 Jul;43(7):2784-2791.

23. Eckle M, Decher G. Tuning the performance of layer-by-layer assembled organic light emitting diodes by controlling the position of isolating clay barrier sheets. Nano Letters 2001 Jan;1(1):45-49.

24. Jang WS, Rawson I, Grunlan JC. Layer-by-layer assembly of thin film oxygen barrier. Thin Solid Films 2008 Jun 2;516(15):4819-4825.

25. Kotov N. Clay nanosheets comprise new material with strength of steel. Materials Performance 2008 Jan;47(1):20-21.

26. Yoo PJ, Nam KT, Qi JF, Lee SK, Park J, Belcher AM, et al. Spontaneous assembly of viruses on multilayered polymer surfaces. Nature Materials 2006 Mar;5(3):234-240.

27. Dawidczyk TJ, Walton MD, Jang WS, Grunlan JC. Layer-by-layer assembly of UV-resistant poly(3,4-ethylenedioxythiophene) thin films. Langmuir 2008 Aug 5;24(15):8314-8318.

28. Sukhorukov GB, Donath E, Lichtenfeld H, Knippel E, Knippel M, Budde A, et al. Layer-by-layer self assembly of polyelectrolytes on colloidal particles. Colloids and Surfaces a-Physicochemical and Engineering Aspects 1998 Jun 15;137(1-3):253-266.

29. Grunlan JC, Choi JK, Lin A. Antimicrobial behavior of polyelectrolyte multilayer films containing cetrimide and silver. Biomacromolecules 2005 Mar-Apr;6(2):1149-1153.

30. Podsiadlo P, Paternel S, Rouillard JM, Zhang ZF, Lee J, Lee JW, et al. Layer-by-layer assembly of nacre-like nanostructured composites with antimicrobial properties. Langmuir 2005 Dec 6;21(25):11915-11921.

31. Fujita S, Shiratori S. Waterproof anti reflection films fabricated by layer-by-layer adsorption process. Japanese Journal of Applied Physics Part 1-Regular Papers Short Notes & Review Papers 2004 Apr;43(4B):2346-2351.

32. Lowman GM, Tokuhisa H, Lutkenhaus JL, Hammond PT. Novel solid-state polymer electrolyte consisting of a porous layer-by-layer polyelectrolyte thin film and oligoethylene glycol. Langmuir 2004 Oct 26;20(22):9791-9795.

33. Antipov AA, Sukhorukov GB, Donath E, Mohwald H. Sustained release properties of polyelectrolyte multilayer capsules. Journal of Physical Chemistry B 2001 Mar 29;105(12):2281-2284.

34. Wood KC, Little SR, Langer R, Hammond PT. A family of hierarchically self-assembling linear-dendritic hybrid polymers for highly efficient targeted gene delivery. Angewandte Chemie-International Edition 2005;44(41):6704-6708.

35. Decher G, Lehr B, Lowack K, Lvov Y, Schmitt J. New Nanocomposite Films for Biosensors - layer-by-layer adsorbed films of polyelectrolytes, Proteins or DNA. Biosensors & Bioelectronics 1994;9(9-10):677-684.

36. Tang ZY, Kotov NA, Magonov S, Ozturk B. Nanostructured artificial nacre. Nature Materials 2003 Jun;2(6):413-U418.

37. Ai H, Jones SA, Lvov YM. Biomedical applications of electrostatic layer-by-layer nano-assembly of polymers, enzymes, and nanoparticles. Cell Biochemistry and Biophysics 2003;39(1):23-43.

38. Dibrov P, Dzioba J, Gosink KK, Hase CC. Chemiosmotic mechanism of antimicrobial activity of Ag+ in Vibrio cholerae. Antimicrobial Agents and Chemotherapy 2002 Aug;46(8):2668-2670.

39. Simonetti N, Simonetti G, Bougnol F, Scalzo M. Electrochemical Ag+ for preservative use. Applied and Environmental Microbiology 1992 Dec;58(12):3834-3836.

40. Becerril R, Gomez-Lus R, Goni P, Lopez P, Nerin C. Combination of analytical and microbiological techniques to study the antimicrobial activity of a new active food packaging containing cinnamon or oregano against e-coli and s-aureus. Analytical and Bioanalytical Chemistry 2007 Jul;388(5-6):1003-1011.

41. Han JH. Antimicrobial food packaging. Food Technology 2000 Mar;54(3):56-65.

42. Quintavalla S, Vicini L. Antimicrobial food packaging in meat industry. Meat Science 2002 Nov;62(3):373-380.

43. Tripathi S, Mehrotra GK, Dutta PK. Chitosan based antimicrobial films for food packaging applications. E-Polymers 2008 Aug 2:-.

44. Sant SB, Gill KS, Burrell RE. Nanostructure, dissolution and morphology characteristics of microcidal silver films deposited by magnetron sputtering. Philod Mag Lett 2000;80:249.

45. Calva J. Antibiotic use in a periurban community in Mexico: A household and drugstore survey. Social Science & Medicine 1996 Apr;42(8):1121-1128.

46. Levy SB. Factors impacting on the problem of antibiotic resistance. Journal of Antimicrobial Chemotherapy 2002 Jan;49(1):25-30.

47. Stewart PS, Costerton JW. Antibiotic resistance of bacteria in biofilms. Lancet 2001 Jul 14;358(9276):135-138.

48. Sondi I, Salopek-Sondi B. Silver nanoparticles as antimicrobial agent: A case study on E-coli as a model for gram-negative bacteria. Journal of Colloid and Interface Science 2004 Jul 1;275(1):177-182.

49. Kenawy ER, Worley SD, Broughton R. The chemistry and applications of antimicrobial polymers: A state-of-the-art review. Biomacromolecules 2007 May;8(5):1359-1384.

50. Chambers HF. Chapter 43. In: J. G. Hardman LEL, A. G. Gilman, editor. Goodman and Gilman's The Pharmacological Basis of Theraputics, 10th ed. New York: McGraw-Hill, 2001.

51. Balogh L, Swanson DR, Tomalia DA, Hagnauer GL, McManus AT. Dendrimer-silver complexes and nanocomposites as antimicrobial agents. Nano Letters 2001 Jan;1(1):18-21.

52. Kumar R, Munstedt H. Silver ion release from antimicrobial polyamide/silver composites. Biomaterials 2005 May;26(14):2081-2088.

53. Redmond SM, Rand SC, Tang HX, Martin DC, Balogh P, Balogh L. Fabrication, characterization, and optical properties of ultrathin dendrimer nanocomposite multilayers containing nanosized metallic silver domains in well structured organic films. Abstracts of Papers of the American Chemical Society 2000 Aug 20;220:U285-U286.

54. Tew GN, Liu DH, Chen B, Doerksen RJ, Kaplan J, Carroll PJ, et al. De novo design of biomimetic antimicrobial polymers. Proceedings of the National Academy of Sciences of the United States of America 2002 Apr 16;99(8):5110-5114.

55. Woo GLY, Mittelman MW, Santerre JP. Synthesis and characterization of a novel biodegradable antimicrobial polymer. Biomaterials 2000 Jun;21(12):1235-1246.

56. Touitou E, Deutsch J, Matar S. Iodine-polyurethane matrices - antimicrobial activity vs method of preparation. International Journal of Pharmaceutics 1994 Mar 15;103(2):199-202.

57. Gottenbos B, van der Mei HC, Klatter F, Nieuwenhuis P, Busscher HJ. In vitro and in vivo antimicrobial activity of covalently coupled quaternary ammonium silane coatings on silicone rubber. Biomaterials 2002 Mar;23(6):1417-1423.

58. Tiller JC, Liao CJ, Lewis K, Klibanov AM. Designing surfaces that kill bacteria on contact. Proceedings of the National Academy of Sciences of the United States of America 2001 May 22;98(11):5981-5985.

59. Donelli G, Francolini I, Piozzi A, Di Rosa R, Marconi W. New polymer-antibiotic systems to inhibit bacterial biofilm formation: A suitable approach to prevent central venous catheter-associated infections. Journal of Chemotherapy 2002 Oct;14(5):501-507.

60. Gu HW, Ho PL, Tong E, Wang L, Xu B. Presenting vancomycin on nanoparticles to enhance antimicrobial activities. Nano Letters 2003 Sep;3(9):1261-1263.

61. Zasloff M. Antimicrobial peptides of multicellular organisms. Nature 2002 Jan 24;415(6870):389-395.

62. Evans DJ, Allison DG, Brown MRW, Gilbert P. Effect of growth-rate on resistance of gram-negative biofilms to cetrimide. Journal of Antimicrobial Chemotherapy 1990 Oct;26(4):473-478.

63. Brown MRW, Collier PJ, Gilbert P. Influence of growth-rate on susceptibility to antimicrobial agents - modification of the cell-envelope and batch and continuous culture studies. Antimicrobial Agents and Chemotherapy 1990 Sep;34(9):1623-1628.

64. Kagan B. Antimicrobial Therapy. 3rd ed. Philadelphia, PA: W. B. Saunders Company, 1980.

65. Petrocci AN. Surface-active agents: Quaternary ammonium compounds. In: Block SS, editor. Disinfection, Sterilization, & Preservation. Philadelphia, PA: Lea & Febiger, 1983. p. 309-329.

66. Hugo W. Some aspects of action of cationic surface active agents in microbial cells with special reference to their action on enzymes. Chemistry & Industry 1965(10):420-&.

67. Denyer SP, Hugo WB. Mode of action of tetradecyltrimethyl ammonium bromide (ctab) on staphylococcus-aureus. Journal of Pharmacy and Pharmacology 1977;29:P66-P66.

68. Jacobs AA, Heidelberger M. The quaternary salts of hexamethylenetetramine. III. monohalogenacylated aromatic amines and their hexamethylenetetraminium salts. Journal of Biological Chemistry 1915 May;21(1):103-143.

69. Jacobs WA, Heidelberger M. The quaternary salts of hexamethylenetetramine. VIII. Miscellaneous substances containing aliphatically bound halogen and the hexamethylenetetraminium salts derived therefrom. Journal of Biological Chemistry 1915 Jun;21(2):465-475.

70. Jacobs WA, Heidelberger M. The quaternary salts of hexamethylenetetramine. VII. omega-halogen derivatives of aliphatic-aromatic ketones and their hexamethylenetetraminium salts. Journal of Biological Chemistry 1915 Jun;21(2):455-464.

71. Jacobs WA, Heidelberger M. The quaternary salts of hexamethylenetetramine. VI. Halogenethyl ethers and esters and their hexamethylenetetraminium salts. Journal of Biological Chemistry 1915 Jun;21(2):439-453.

72. Jacobs WA, Heidelberger M. The quaternary salts of hexamethylenetetramine. V. Monohalogenacetyl derivatives of aminoalcohols and the hexamethylenetetraminium salts derived therefrom. Journal of Biological Chemistry 1915 Jun;21(2):403-437.

73. Jacobs WA, Heidelberger M. Quaternary salts of hexamethylenetetramine. IV. Monohalogenacylated simple amines, ureas, and urethanes, and the hexamethylenetetraminium salts derived therefrom. Journal of Biological Chemistry 1915 May;21(1):145-152.

74. Jacobs WA, Heidelberger M. The quaternary salts of hexamethylenetetramine. II. Monohalogenacetylbenzylamines and their hexamethylenetetraminium salts. Journal of Biological Chemistry 1915 Apr;20(4):685-694.

75. Jacobs WA, Heidelberger M. The quaternary salts of hexamethylenetetramine. I. Substituted benzyl halides and the hexamethylenetetraminium salts derived therefrom. Journal of Biological Chemistry 1915 Apr;20(4):659-683.

76. Domagk G. A new class of disinfectant. Deutsche Medizinische Wochenschrift 1935;61:829-832.

77. Zana R. Dimeric and oligomeric surfactants. Behavior at interfaces and in aqueous solution: A review. Advances in Colloid and Interface Science 2002 Mar 29;97(1-3):205-253.

78. Zhu P, Sun G. Antimicrobial finishing of wool fabrics using quaternary ammonium salts. Journal of Applied Polymer Science 2004 Aug 5;93(3):1037-1041.

79. Jones RD. Bacterial resistance and topical antimicrobial wash products. American Journal of Infection Control 1999 Aug;27(4):351-363.

80. Jana NR, Gearheart L, Murphy CJ. Wet chemical synthesis of high aspect ratio cylindrical gold nanorods. Journal of Physical Chemistry B 2001 May 17;105(19):4065-4067.

81. Jana NR, Gearheart L, Murphy CJ. Wet chemical synthesis of silver nanorods and nanowires of controllable aspect ratio. Chemical Communications 2001(7):617-618.

82. Athawale AA, Katre PP, Kumar M, Majumdar MB. Synthesis of CTAB-IPA reduced copper nanoparticles. Materials Chemistry and Physics 2005 Jun 15;91(2-3):507-512.

83. Krishnaswamy R, Pabst G, Rappolt M, Raghunathan VA, Sood AK. Structure of DNA-CTAB-hexanol complexes. Physical Review E 2006 Mar;73(3):-.

84. Brown GM, Butler JH. New method for the characterization of domain morphology of polymer blends using ruthenium tetroxide staining and low voltage scanning electron microscopy (LVSEM). Polymer 1997 Jul;38(15):3937-3945.

85. Schlenoff JB, Ly H, Li M. Charge and mass balance in polyelectrolyte multilayers. Journal of the American Chemical Society 1998 Aug 5;120(30):7626-7634.

86. Benson HJ. Microbiological applications a laboratory manual in general microbiology. 3rd ed. Duboque, IA: Wm. C. Brown Company Publishers, 1980.

87. Powers JH. Antimicrobial drug development - the past, the present, and the future. Clinical Microbiology and Infection 2004 Nov;10:23-31.

88. Mendelsohn JD, Yang SY, Hiller J, Hochbaum AI, Rubner MF. Rational design of cytophilic and cytophobic polyelectrolyte multilayer thin films. Biomacromolecules 2003 Jan-Feb;4(1):96-106.

89. Balabushevitch NG, Sukhorukov GB, Moroz NA, Volodkin DV, Larionova NI, Donath E, et al. Encapsulation of proteins by layer-by-layer adsorption of polyelectrolytes onto protein aggregates: Factors regulating the protein release. Biotechnology and Bioengineering 2001 Nov;76(3):207-213.

90. Caruso F, Trau D, Mohwald H, Renneberg R. Enzyme encapsulation in layer-by-layer engineered polymer multilayer capsules. Langmuir 2000 Feb 22;16(4):1485-1488.

91. Trau D, Renneberg R. Encapsulation of glucose oxidase microparticles within a nanoscale layer-by-layer film: immobilization and biosensor applications. Biosensors & Bioelectronics 2003 Oct 15;18(12):1491-1499.

92. Reisner E, Fontecilla-Camps JC, Armstrong FA. Catalytic electrochemistry of a [NiFeSe]-hydrogenase on TiO2 and demonstration of its suitability for visible-light driven H-2 production. Chemical Communications 2009(5):550-552.

VITA

Name: Charlene Myriah Dvoracek

Address: Department of Mechanical Engineering
c/o Dr. Jaime Grunlan
Texas A&M University
College Station, TX 77843-3123

Email Address: charlidvoracek@gmail.com

Education: B.S., Mechanical Engineering, Rose-Hulman Institute of Technology, 2007

M.S. Mechanical Engineering, Texas A&M University, 2009